Solid lipid nanoparticles for ocular delivery of isoniazid: evaluation, proof of concept and invivo safety & kinetics.

Journal:	*Nanomedicine*
Manuscript ID	NNM-2018-0278
Manuscript Type:	Research Article
Keywords:	Solid lipid nanoparticles, Ocular tuberculosis, Isoniazid

Abstract:

Aim: Evaluating solid lipid nanoparticles (INH-SLNs) for ocular delivery of isoniazid.

Materials & methods: Characterized of INH-SLNs for morphological, thermal, crystallinity and NMR studies. *In vitro* release and *ex-vivo* corneal permeability studies were conducted. Proof-of-concept uptake studies using fluorescein-labelled SLNs (F-SLNs), in corneal and conjunctival cell lines and in eye. Antimycobacterial activity of INH-SLNs was confirmed. In vivo aqueous humor pharmacokinetics, toxicity and tolerance was performed in rabbit eye.

Results: INH-SLNs showed extended release (48 h); enhanced corneal permeability (1.6 times); 5 times lower MIC; significant uptake of F-SLNs in corneal and conjunctival cells and ocular tissues; 4.2 times improvement in ocular bioavailability (AUC) and *in vivo* acute and repeat dose safety.

Conclusion: INH-SLNs is an effective ocular delivery system.

Introduction

Tuberculosis (TB) is an airborne infectious disease caused by *Mycobacterium tuberculosis* which commonly affects the lungs. Extrapulmonary TB including orbital and external eye disease, represented 15% of 6.3 million cases that were notified in 2016 [1]. The precise incidence of ocular TB is however difficult to discern; ranging from 1.4% to 18% in various studies [2-4]. Ocular TB may primarily be a result of direct inoculation and or due to entry of the Mycobacterium into ocular surface and also delayed hypersensitivity reaction to the Mycobacterium protein [5]. TB of the eyes mostly affects the ciliary body and choroid due to the high regional oxygen tension of these tissues. Uveitis, especially posterior uveitis, is the most common form of intraocular TB. The most common clinical presentation appears to be posterior uveitis, followed by anterior uveitis, panuveitis, and intermediate uveitis [6]. Due to the complex nature of the eye including various anatomical and physiological barriers, significant challenges are involved in its treatment [7]. Presently the ocular TB treatment is similar to the systemic treatment option which involves 6-month oral therapy of four first-line drugs: isoniazid, rifampicin, ethambutol and pyrazinamide [8]. No better agent than the available options has been discovered for TB in the recent past, despite significant efforts.

Isoniazid (INH) is a potent bactericidal agent and the most frequently used candidate for ocular TB treatment and recommended by WHO for the management of all forms of TB. It is a Biopharmaceutical Classification System (BCS)-class III drug (high solubility and low permeability) showing an aqueous solubility of 140 mg/ml and log P of -0.64. It However, hepatotoxicity and neurotoxicity associated with its systemic and prolonged use is a concern [9] .

The most logical option to overcome these undesired systemic side effects of INH is to deliver the drug locally to the eye. However, the highly impermeable milieu of the eye especially the corneal surface and the factors like pre-corneal loss due to blinking, rapid washout by tears, drainage through the naso-lacrimal duct, and non-productive absorption limit successful therapy.

Solid lipid nanoparticles (SLNs) have attracted an enormous interest in recent years as an ocular drug delivery option. In our previous works, we developed INH-SLNs which

modified the pharmacokinetic distribution of INH in plasma and brain following oral administration [10]. A 6 times improvement in plasma bioavailability and 4 times increase in brain bioavailability was observed with respect to free drug.

Presently INH-SLN was evaluated for its suitability to deliver INH in to the eye following topical application as drops. The drug loading of INH in presently prepared SLNs was increased to 40% with respect to the lipid matrix to produce a concentrated dispersion which can deliver significant amount in a drop. *In vitro* release, *ex vivo* corneal permeability, and *in vivo* ocular pharmacokinetic profile of INH-SLNs was compared with the corresponding free drug solution. A fluorescein-labelled SLN system was used to confirm capacity of developed SLNs to reach internal eye tissues. The uptake of developed SLN formulation into corneal and conjunctival cells was also confirmed. AFM, TEM, DSC, FTIR, XRD and NMR studies in addition to particle size and zeta potential determination were done to describe the developed INH-SLN system.

Two tier safety as (i) cytotoxicity and (ii) *in vivo* (a) acute dose and (b) 7 days repeat-dose ocular toxicity (following dermal toxicity) was established in rabbits, as per OECD guidelines. Stability studies were also conducted on the aqueous INH-SLN dispersions.

MIC and in vitro antimycobacterial activity of INH-SLNs versus free INH was also determined.

Materials and methods

Materials

Isoniazid was bought from Sigma Aldrich USA, and soy lecithin (Phospholipon® 90H) was received as a gift sample from Lipoid GmbH, Germany. Compritol 888 ATO® was a gift sample from Gattefosse India Pvt Ltd. Stearic acid and Tween 80 were purchased from Central Drug House, Mumbai. All other chemicals and solvents used in the study were of analytical or HPLC grade.

Methods

Preparation of INH-SLNs

Solid lipid nanoparticles of isoniazid (INH) were prepared by the microemulsification method [11]. Briefly the lipidic phase (Compritol 888 ATO® and Stearic acid (4:1) – Combi lipid) and the aqueous phase (polysorbate 80, soy lecithin and water) containing dissolved INH were heated to ~10°C above the lipid melt temperature.

The proportion of surfactant and the volumes of two phases were so adjusted that a microemulsion was formed spontaneously upon mixing the two phases. Hot microemulsion, thus formed was transferred to an equal volume of cold water (~2°C) under constant stirring (WiseTis HG-15 D, 10,000 rpm) to obtain SLNs. The prepared SLNs were used as such for further studies without dialysing the unentrapped INH.

Note: - Fluorescein sodium loaded SLNs (F-SLNs) were also prepared similarly except that INH was replaced with fluorescein sodium. Free fluorescein was removed from the system by dialysis prior to application.

In vitro release studies

In vitro release was performed using a glass tube open at both the ends with a dialysis membrane tied on its one side. A fixed quantity (3 ml) INH-SLNs or INH solution (INH-SOL), equivalent to 40 mg INH, was loaded on the dialysis membrane inside of the tube. This side of the tube (donor side) was dipped in 80 ml of dialysate comprising pH 7.2 phosphate buffer (20 mM) at 37 ºC. The dialysis membrane (12000 cut-off) was soaked in distilled water for 12 h prior to use. Suitable aliquots (3 ml) of dialysate were withdrawn from time to time and replaced with fresh solution. The samples were quantified by HPLC, as described below in section. The cumulative drug released was calculated and expressed as a percentage of the theoretical maximum drug content. Model fitting was performed in order to select the best fit model describing the release of INH from its SLN dispersion.

Ex-vivo, porcine cornea permeability studies

Freshly procured porcine cornea was mounted on a previously described diffusion cell [12]. The receptor compartment comprised of freshly prepared glutathione bicarbonate ringer (GBR) as the diffusion medium (20 ±2 ml), stirred continuously (50 rpm) at 37±0.2 ^{o}C. INH-SLNs and INH-SOL (aqueous solution of pristine INH at same concentration as INH-SLNs) (0.5 ml) placed on the porcine cornea represent the donor side. Samples were withdrawn at various time points with replacement and were analyzed by the developed HPLC method after suitable dilution. The apparent corneal permeability coefficient (Papp) and steady state flux of both INH-SLNs and INH-SOL were determined, as reported previously [13].

Stability study

INH-SLNs was stored in tightly closed, screw capped vials, at 2-8 ºC for 6 and 12 month. Samples were withdrawn and analyzed for particle size, total drug content, FTIR, XRD and DSC.

Proof-of- concept studies: confocal microscopy

A drop (30 µl) of the fluorescein labelled SLNs (F-SLNs) was administered into the fornix of the right eye of rats. Animals were sacrificed at 15 min, 4 h, 8 h and 24 h post instillation of the formulation. Eyes were enucleated immediately and stored at -20 °C. The eyes were embedded in cryomatrixTM before sectioning, and the samples were sliced into 10 µm thick sections using a cryostat (IEC Minotome 3398, American Instrument Exchange, Inc., Massachusetts, USA). Sections were then fixed onto slides. The complete eye sections were observed under confocal microscope (Nikon A1R, Japan) in fluorescent mode (Olympus FV3000) using 1.5X and 10X objective, and a 60X oil immersion objective. The images were processed by NIS-viewer software and fluorescent intensity was obtained using image J software.

Cellular uptake studies

Stratified HCLE (human corneal-limbal epithelial), and HCJE (human conjunctival epithelial) cell lines were maintained in 50% Dulbecco's Modified Eagles Medium (DMEM) and 50% F12 medium supplemented with 10% fetal calf serum (FCS), 100 U/ml penicillin G and 100 µg/ml streptomycin, in a humidified incubator at 37 °C in 5% CO_2. Cells were grown on coverslip and incubated with fluorescein labelled SLNs (F- SLNs), and an equivalent free fluorescein solution in standard medium for 2 h. Cells were then washed, fixed and coverslips mounted according to routine immunocytochemistry methods.

Minimum inhibitory concentration

Minimum inhibitory concentration (MIC) of INH, Blank-SLNs and INH-SLNs was determined against *M. tuberculosis* H37Rv (ATCC 25618). Sterile agar media was mixed with 2 ml of *M. tuberculosis* H37Rv (2.5×10^7 CFU/ml) containing various concentrations of free INH or Blank or INH-SLN formulations. The mixture was poured into 85 mm diameter petri dishes (approx. 30 ml each) and allowed to

solidify. All serial dilutions were made using sterile milli-Q water. The MIC was determined as lowest concentration causing no visible growth of H37Rv after incubation.

Susceptibility test against *M. tuberculosis*

M. tuberculosis H37Rv was grown to logarithmic phase (equivalent to OD_{595} ~ 0.5) in Middlebrook 7H9 broth (Difco Laboratory, USA) supplemented with albumin dextrose complex (Difco Laboratory, USA) for stock preparation. The bacterium was sub-cultured under aerobic condition in the same media from the stock at 37 ºC. Susceptibility test was performed by proportion method as reported earlier with slight modification [14, 15]. This method determines the percent growth (number of colonies) of a defined inoculum on control media (free from drug) versus growth of culture on media containing test sample (in critical amount) supposed to inhibit tuberculosis strain Rv. LJ media was inoculated (one loopful equivalent to 6.0 µl) with previously grown culture and incubated at 37 ºC for 6 weeks. Isolated colonies were picked and dispersed in water for injection (2 ml) to achieve a suspension equivalent to McFarland standard 1.0. The suspension was vortexed for 1 min to get a homogeneous culture and left for some time to remove any entrapped air bubbles. Standard dilution of 10^{-4} was prepared to inoculate the LJ media contained in McCartney vial. Control vial and vial containing SLNs were inoculated with same dilution (10^{-4}) and incubated overnight in a slant position with loosened cap at 37 ◦C. After 12 h of incubation (overnight), the cap was tightened and incubation was continued for period of 6 weeks in upright position, although susceptibility was also assessed on 28th day. The absence of colonies will confirm susceptibility of Rv strain to the treatment. The experiment was performed in Class II Biological Safety Cabinet and taking all care of infection.

High performance liquid chromatography (HPLC) analysis of Isoniazid

The determination of INH was carried out using a HPLC system (waters, alliance separation module e2695). A reversed phase X Bridge™ C_{18} column (250 mm × 4.6 mm, 5 µm; Waters, USA) was used. Phosphate buffer solution (20 mM)/Acetonitrile (98:2, isocratic) was run as the mobile phase. The elution was performed at a flow rate of 1.0 ml/min and the analytical column was kept in a thermostated oven at 35 ºC. The detection of INH was performed with Waters 2998 Photodiode Array

Detector at a set wavelength of 261 nm. The injection volume was 20 µl for all standards and samples. INH was eluted approximately 5.4 min after injection. A series of standard solutions of INH (100–1600 ng/mL) were prepared in milli Q water. The assay was linear ($R^2 > 0.99$) for INH over the concentration range of 200–1600 ng/ml.

Bioanalytical Method validation

Method validation of INH in aqueous humor was carried out, following US Food and Drug Administration guidelines add year. The method was validated for system suitability, specificity, sensitivity, recovery, precision and accuracy, linearity and matrix effect of INH during sample processing.

Preparation of the calibration curve in aqueous humor

A five point calibration curve of INH was prepared by spiking 40 µl of blank aqueous humor with 10 µl each of the appropriate working dilution of INH to result in 600 to 1600 ng/ml of INH.

High quality control (HQC: 1600 ng/ml), medium quality control (MQC: 1200 ng/ml) and low quality control (LQC: 800 ng/ml) samples were prepared similarly for validation.

System suitability

System suitability was performed by determining AUC for the MQC (without spiking into aqueous humor) sample injected into the HPLC before the start of each analytical run and its comparison with the average AUC value obtained for the MQC, upon repetitive injections.

Specificity

Blank aqueous humor samples were prepared according to the sample preparation procedure described in experimental section. and screened for the presence of any interfering peaks corresponding to or near to the retention time of INH.

Sensitivity

The limit of quantification (LOQ) was taken as the lowest concentration in the standard curve with accuracy between 80–120%

and limit of detection (LOD) was determined at a signal to noise ratio (S/N) of 3 [16].

Recovery

Recovery pertains to the extraction efficiency of an analytical method within the limits of variability. Recovery experiments was performed by comparing the analytical results for extracted samples at three concentrations (800, 1200, and 1600 ng/ml) with the corresponding standards.

Inter-day and intra-day precision and accuracy

Inter-day and intra-day precision and accuracy were evaluated by spiking known concentration of INH in aqueous humor. The precision was expressed as % CV (coefficient of variation) and % accuracy was expressed by using the formula: measured concentration/nominal concentration × 100.

Three different concentrations (LQC, MQC and HQC) were used and samples were prepared as per the procedures described above. Inter-day precision and accuracy were assessed over a period of 3 days using replicate (n=6) determinations for the spiked aqueous humor samples, whereas intra-day precision and accuracy were assessed on three separate occasions on the same day (n=6) for each concentration respectively.

Pharmacokinetic studies

Study design

Male rabbits, weighing approximately 1.5 kg, were purchased from IMTECH (Chandigarh, India). Prior to experiments the rabbits were housed in standard cages and allowed free access to food and water. All the animal study protocols were approved by the Institutional Animals Ethics Committee, PU, Chandigarh (vide letter no. PU/IAEC/S/14/90). A total of 12 rabbits were used for the study. INH-SOL (n=6) and INH-SLNs (n=6) (150 µl** each; 150 µl x 14.32 mg/ml= 2.14 mg of INH) were instilled into one eye of each rabbit, keeping the other eye as control. Aqueous humor from dosed eye was withdrawn at 0.25, 0.5, 1, 2, 4, 8, 12, 24 and 48 h. The samples were collected and processed as described below.

Aqueous humor from contralateral eye was also collected at some time points to confirm any systemic drainage of INH.

** *Five 30 µl drops at 5 min intervals (150 µl) were instilled into each eye. Time of instilling last drop was taken as 0 time.*

Aqueous humor sampling

After topical anaesthesia, the 26-gauge needle was inserted, just above the cornea-sclera limbus, so as to traverse through the centre of anterior chamber to withdraw aqueous humor. Around 100 µl of aqueous humor was withdrawn from each eye at every time-point. The aqueous humor was collected in polypropylene tubes and was labelled and stored at −20 °C until further analysis.

Sample preparation (extraction procedure)

To 50 µl of aqueous humor samples in an eppendorf tube, 450 µl of chloroform: methanol (3:1) was added. The sample was vortexed for 5 min and centrifuged at 15,000 rpm to separate precipitated proteins. Supernatant, transferred to suitably labelled tubes, was evaporated to dryness on SPD speed Vac (Thermo Saavant add country etc) at a temperature of 50 ºC for 2 h; this step was repeated twice and the dried sample was reconstituted with 500 µl of MilliQ water. The sample was filtered through 0.2 µm syringe filter and was used for analysis using the developed HPLC method. Each sample was internally spiked with 4 µg/ml of INH so as to ensure detection of concentrations below limit of quantification (LOQ). All the conditions of HPLC were maintained the same as discussed earlier in section.

Data Analysis

The pharmacokinetic parameters were calculated using non-compartmental model. The area under the concentration–time curve from time zero to time t (AUC_{0-t}) was calculated using the trapezoidal method. Peak concentration (C_{max}) and the time at which the peak concentration is achieved (T_{max}), were obtained directly from the individual concentration-time profiles. All values were corrected for the spiked concentration. The area under the concentration-time curve from time zero to infinity was calculated by: $AUC_{0-\infty} = AUC_{0-t} + C_t/K_e$, where C_t is the drug concentration observed at the last time and K_e is the apparent elimination rate constant obtained from the terminal slope of the individual concentration-time curves after logarithmic transformation of the concentration values and application of linear regression. The data obtained from pharmacokinetic parameters were

analyzed for statistical significance by a one way analysis of variance (ANOVA) followed by the Tukey's test.

Results and Discussion

Preparation and characterization of INH-SLNs

The INH-SLNs were prepared successfully and repetitively (n=6) by the microemulsion technique using Combi lipid, as the lipid core material and at a drug loading of 40% with respect to the lipid matrix. The samples were used as such without any further processing (viz. removing the free unentrapped drug from the samples) for all characterisation and evaluation parameters.

Stability studies

No significant change ($p<0.05$) in entrapment efficiency, total drug content and particle size of INH loaded SLN dispersion was observed upon storage under refrigeration for 6 months and 12 months, confirming their long term stability (Table 1).

Table 1 Stability study at 4±3 ^{o}C (n=6)

% Change in parameters			
Time (months)	**INH-SLNs**		
	TDC %	**EE %**	**Particle size**
0	91.6 ± 3.40	65.2 ± 1.32	149.2 ± 4.90
6	89.61± 2.90	64.75±0.87	153.8±8.60
12	91.4 ± 4.64	66.4 ± 1.32	152.0 ± 0.18

Values are mean ± standard deviation. The results were analysed for statistical significance by a t test Values were not significantly different from one another, at p <0.05.

Most nanostructured systems are recommended to be dialysed or lyophilized to retain their stability on storage. Such methods are (i) costly, (ii) time consuming (iii) may result in aggregates and microsized particles on reconstitution, and (iv) change the native milieu of nanoparticles, which may destabilize the system. The prepared aqueous SLN dispersion was stable for 1 year at 4 ºC. This may be attributed to the maintenance of SLNs in their native state in which they were produced [17] comprising suitable concentration of surfactants in the aqueous phase in which they remain dispersed even on long term storage.

In vitro release

The release of drug from a matrix can be predicted based on the various drug release models and the release pattern can indicate the drug incorporation models.

Five possible methods of drug release from SLNs is reported in the literature which are (a) desorption of drug bound to the surface, (b) diffusion through the nanoparticle matrix, (c) diffusion through the wall of nanocapsules, (d) nanoparticle matrix erosion, or (e) a combined erosion–diffusion process.

Depending on the type of drug, incorporated amount, types and amounts of excipients, preparation technique and, environmental conditions during drug release as well as the geometry and dimensions of the nanoparticle, the drug release phenomenon may vary.

The in vitro release profile of INH-SOL and INH-SLNs was obtained by the dialysis bag technique using simulated tear fluid (pH 7.2). All the INH from dialysis bag was released within 8 hours while INH-SLNs followed an extended released of upto 48 h (Figure 1) at which time 94% of the total INH was released.

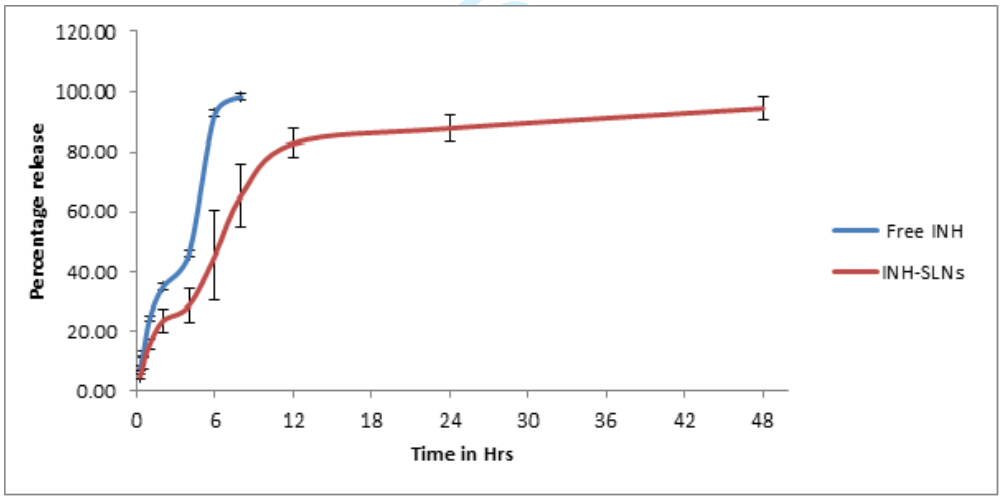

Figure 1: In vitro drug release of INH and INH-SLNs in simulated tear fluid (pH 7.2).

INH release increased exponentially and rapidly in the first 6 h (henceforth referred to as the "initial" release) from SLNs followed by a slower release over 48 h (henceforth referred to as the "sustained" release phase). It may however be noted that 28% drug is released at 4 h and 45% at 6 h. These values closely correspond to the free/unentrapped

drug present in the INH-SLN formulation. What is interesting is the fact that even this free/unentrapped INH is released from the SLNs at a rate much slower (though in a similar pattern) than the pristine drug, indicating that probably this amount is also loosely associated with the SLN particles.

To suggest the mechanism of drug release, various release kinetic models were fitted to the obtained results. For the initial 8 h the Korsemeyer-peppas release model was the best fit model for both free INH and INH-SLNs. Peppas release exponent, n value, was 0.85 indicating that the release of INH was governed by an "anomalous" process or non fickian diffusion. The anomalous transport could include both the drug diffusion and matrix swelling [18]. From 12 h to 48 h this diffusion controlled release was predicted to occur from a porous matrix as indicated by the Higuchi model. It seems that particles of drug closest to the surface of SLNs i.e. SLN shell are dissolved rapidly, generating numerous pores. Drug lying/entrapped within the core then diffuses to the surface and passes into the medium through pores the pores created on the surface such a mechanism is indicated for hydrophilic drugs. The factors affecting INH release form SLNs include presence of free drug in the surfactant coat as per its aqueous solubility and the later sustained release phase (8 h onwards) was due to the adsorption and encapsulation of drug within the lipid core.

Ex-vivo corneal permeation

INH-SLNs showed a significant improvement in apparent permeation coefficient (P_{app}) (2.2 fold), total amount permeated (1.6 fold) and percentage drug permeated (2.5 fold) at 6 h as compared to free INH (INH-SOL) taken as control (Table 2; Figure 2). Ex-vivo corneal permeation studies showed a significant improvement in flux (1.7 times) and total amount of INH permeated (0.24 mg/hr/cm^2; 154 µg) when applied as INH-SLNs versus INH-SOL (0.14 mg/hr/cm^2; 91.0 µg). This enhanced permeation is due to the nanosize (149.2 nm) and composition of SLNs.

The main characteristic of the epithelium is the presence of intercellular tight junctions (zonula occludens) that prevent the diffusion of hydrophilic macromolecules with size > 100 Da through the paracellular route [19]. In contrast, lipophilic substances, which readily diffuse through the lipid-based cell membranes, can pass through the epithelium via a transcellular route. The epithelial cells then act as reservoirs that slowly release these substances to the corneal stroma, indicating the feasibility of paracellular transport of developed INH-SLNs [20].

SLN formulation of INH showed high corneal transport. Latter can be attributed (i) encapsulation of INH into the lipophilic SLNs which would facilitate their transcellular transport through the cornea, (ii) presence of a (polysorbate 80), surfactant also helps in enhanced permeation. Latter may also have inhibitory effects on some drug efflux transporters (P-glycoproteins) [21, 22]. (3) Furthermore, the particulate nature of the formulation would ensure its adherence to the ocular surface and prevent tear washout of the drug. This will result in a sustained absorption and effect.

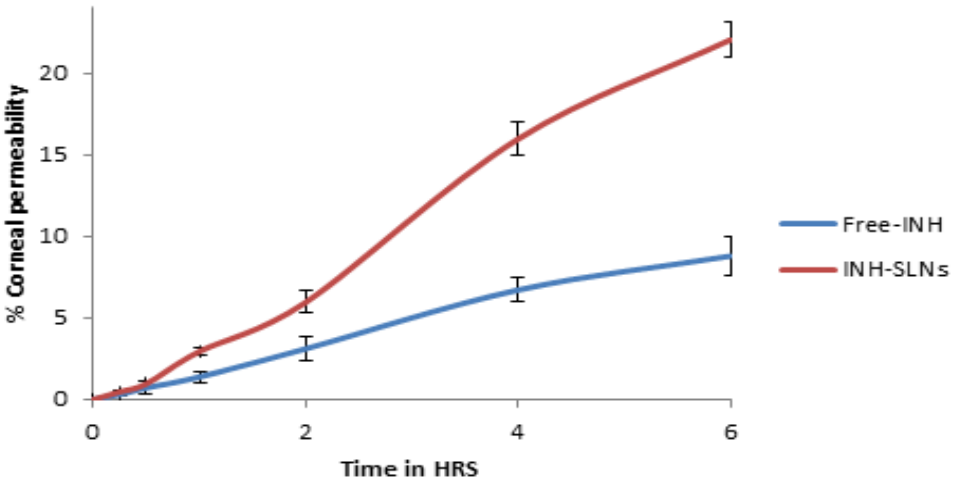

Figure 2: Percentage amount of INH-SLNs and INH-SOL permeated through porcine cornea at various time intervals (n = 6).

Table 2: Comparison of INH-SLNs with INH-SOL, in terms of total amount permeated, percentage permeation, steady state flux and apparent permeability coefficient (Papp) obtained during ex-vivo permeation studies using porcine cornea (n = 6).

Formulation	Total amount permeated in 6 h (µg)	% Permeation	Steady state flux (mg/hr/cm^2)	Apparent permeability coefficient Papp (cm/s)
INH-SOL	91.0 ± 0.12	8.78 ± 1.20	0.14 ± 0.02	3.76 ± 0.53
INH-SLNs	154.0 ± 0.08	22.04 ± 1.12	0.24 ± 0.01	8.17 ± 3.52

Values are mean ± standard deviation. All the values between the two groups were significantly different from one another, at $p < 0.001$, as per t- test

Minimum Inhibitory Concentration

The MIC values of INH, and INH-SLNs were found to be 0.5±0.01, and 0.098±0.003 µg/ml respectively, against *M. tuberculosis* H37Rv (ATCC 25618) whereas the Blank-

SLNs did not show any inhibition at the tested concentrations (Table 3). The MIC value of INH loaded SLNs was ~ 5 times less than INH-SOL. This further increased to 7.1 times if free INH was removed from the SLNs. It may be concluded as also shown earlier that INH-SLNs enhance permeability of INH and hence the susceptibility of *M. tuberculosis* H37Rv to INH. MIC studies were also conducted on Blank-SLNs to ensure that the antibacterial effect was attributable to the INH in INH-SLNs and not to the nanocarrier itself.

The strong antimycobacterial effect of INH-SLNs as compared to pristine INH also indicates enhanced uptake and intracellular retention by the Mycobacterium. The efflux inhibitor property of SLNs has also been suggested to increase the efficacy of drugs by increasing the amount of drug within the bacterial cells.

Table: 3 Results of in vitro anti-tubercular assessment (MIC values) against *Mycobacterium tuberculosis* H37Rv by CFU (colony forming unit/ml) technique.

Minimum Inhibitory Concentration	
Formulation	*M. tuberculosis* H37Rv (ATCC 25618)
INH*	0.5±0.01
Blank-SLNs	-
INH-SLNs (with free drug)**	0.098±0.003
INH-SLNs (without free drug)**	0.07±0.003

(-) No inhibition; Values are mean ± SD (mm) from the experiments in triplicate; Values of INH were significantly greater than those obtained for INH-SLNs, at p < 0.001 when t-test was applied.
**** Values were significantly different from one another, at p <0.001 when t-test applied**

Susceptibility of *M. tuberculosis* H37Rv

Pristine INH, Blank-SLNs and INH-SLNs were appraised for the anti-tubercular activity using tubercular strain H37Rv. After 6 weeks of incubation period, the vials were visualized for any growth of the colonies at the tested concentrations. A dramatic decline in the number of colonies was observed at MIC. Blank-SLNs as expected did not show any inhibition as compared to positive control.

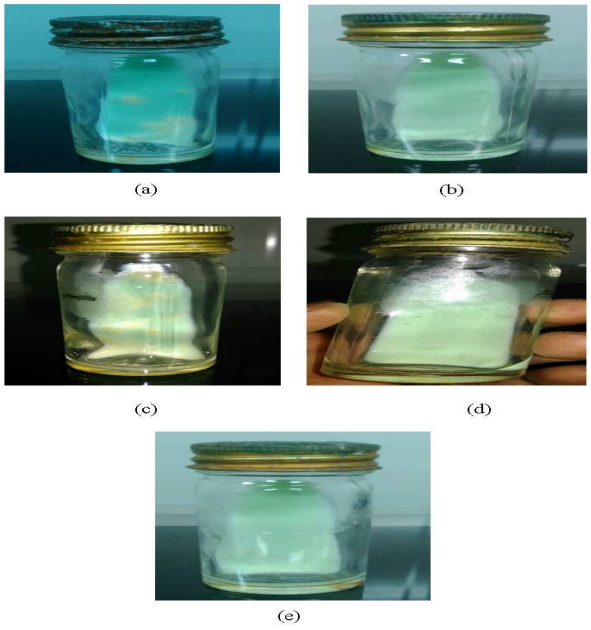

Figure 3: Susceptibility of *M. tuberculosis* H37Rv *to kill*. Control group (a), INH (b), Blank-SLNs (c), INH-SLNs (d), INH-SLNs (without free drug) (e).

Mycobacterium tuberculosis, rely on lipids and on lipid membrane properties to gain access to their host cells, to persist in them (this also assigns resistance to them) and ultimately to egress from their hosts. Several mechanisms may be invoked to explain the influence of lipids on host-pathogen interactions during the various steps in the life cycle of *M. tuberculosis* [23]. To persist inside the phagosome, *M. tuberculosis* depends on host cholesterol. It has been shown that the mycobacterium uses cholesterol/ lipids either as an energy source or as a source of carbon [24].

Hence the lipid based carrier, presently the SLNs, will attract the mycobacterium considering it a substrate. Once the lipid matrix of SLNs is degraded by the lipases produced by the mycobacterium, the encapsulated INH will be released right in its vicinity, producing an effective antibacterial action [25].

Cellular uptake

The intracellular delivery of SLNs was followed first from the interaction of SLN with the cell membrane and then further uptake by the corneal and conjunctival cells. Fluorescein labelled SLNs was used to examine their ability to cross the cell membrane. In order to confirm the uptake, human conjunctival epithelium (HCJE) and human

corneal-limbal epithelial (HCLE) cells were incubated for 2 h with free fluorescein solution (F-SOL) and fluorescein loaded SLN (F-SLNs) (both were of same concentration) and the fluorescence intensity was measured by spectrofluorimeter after lysis of the cells (Figure 4). The control reading confirms that the cellular components itself do not show fluorescence that could potentially interfere with the results. A significantly higher uptake of F-SLNs in HCJE (1218.71 au and 10 times, respectively) and in HCLE cells (1166.21 au and 10.8 times, respectively), in comparison to F-SOL, was observed, establishing that SLNs impart an improved permeability to INH.

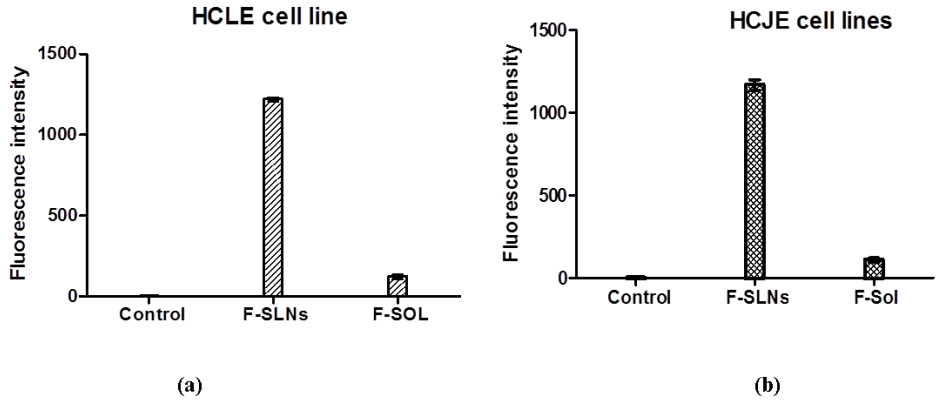

Figure 4: Fluorescence intensity in HCLE (a) and HCJE (b) cells after incubation for 2h

Ocular tissue distribution and fluorescence intensity

It is generally observed that a topically dosed drug can transport to the interior of the eye via: (1) the transcorneal route which can be divided further into a) transvitreous route- where drug diffuses through the cornea, and enters the aqueous and the vitreous cavity; b) the uvea–scleral route where drug diffuses through the cornea, penetrates the aqueous humor, and continues through the uvea-scleral pathway and gains access to the choroid and retina; and the (2) periocular route (conjunctival uptake), where diffusion and absorption occurs via sclera.

In present study the ocular drug distribution from SLNs was determined using fluorescein labelled SLNs (F-SLNs) and compared with fluorescein solution (F-SOL). The ocular sections were viewed under confocal microscope following their application

as drops. Overlay and confocal images confirm the presence of fluorescence upto 24 h after instillation of F-SLNs confirming significant and longer retention of the developed system in the ocular tissues including the internal eye tissue (Figure 5). Whereas the F-SOL shows much lesser fluorescence intensity as compared to F-SLNs (Figure 6).

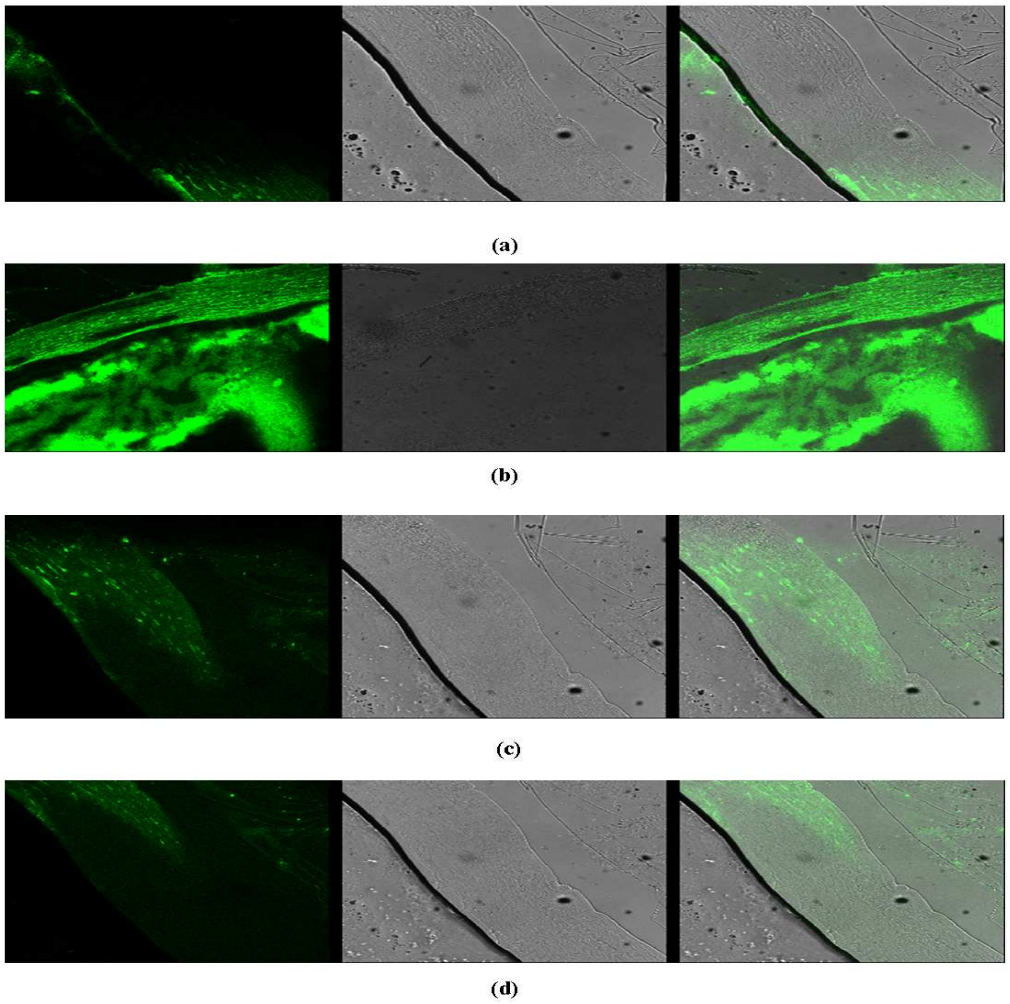

Figure 5: Confocal images of ocular tissues 15 min (a), 30 min (b), 4h. (c), and 24h (d) after topical application of F-SLNs. What do different panels indicate First panel shows fluorescent image, middle panel shows image under bright light, and the last panel shows the overlay image.

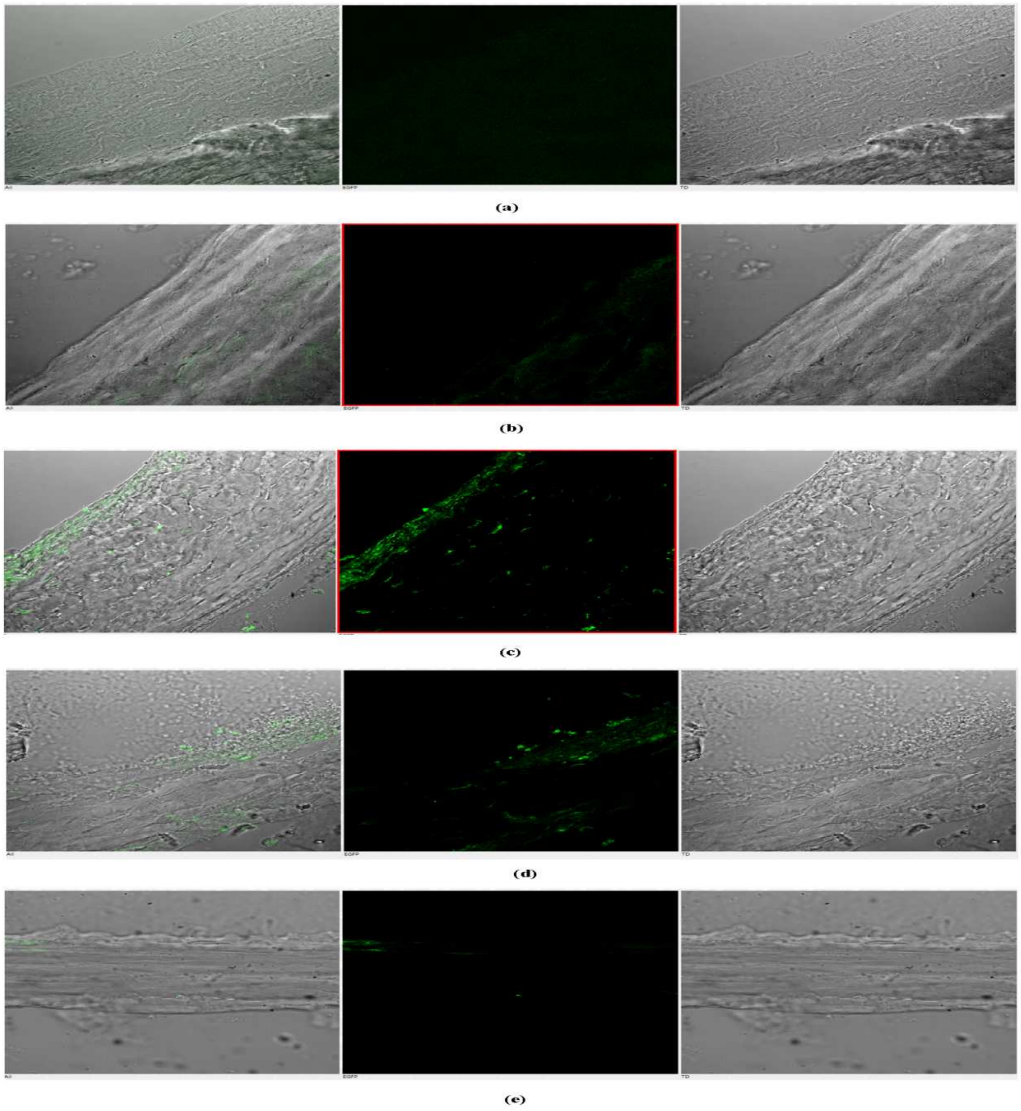

Figure 6: Confocal images of ocular tissues 15 min (a), 30 min (b), 4 h (c), and 24 h (d) after topical application of F-SOL. First panel shows fluorescent image and last panel shows image under bright light, middle panel shows the overlay image.

Table 4: Fluorescent intensity of F-SOL and F-SLNs by using image J software

Time (h)	Intensity of F-SOL	Intensity of F-SLNs
0.25	2.30±4.23	9.88±12.65
0.5	12.67±13.99	35.57±23.91
4	1.30±4.9	12.90±10.15
24	2.69±7.08	13.60±9.11

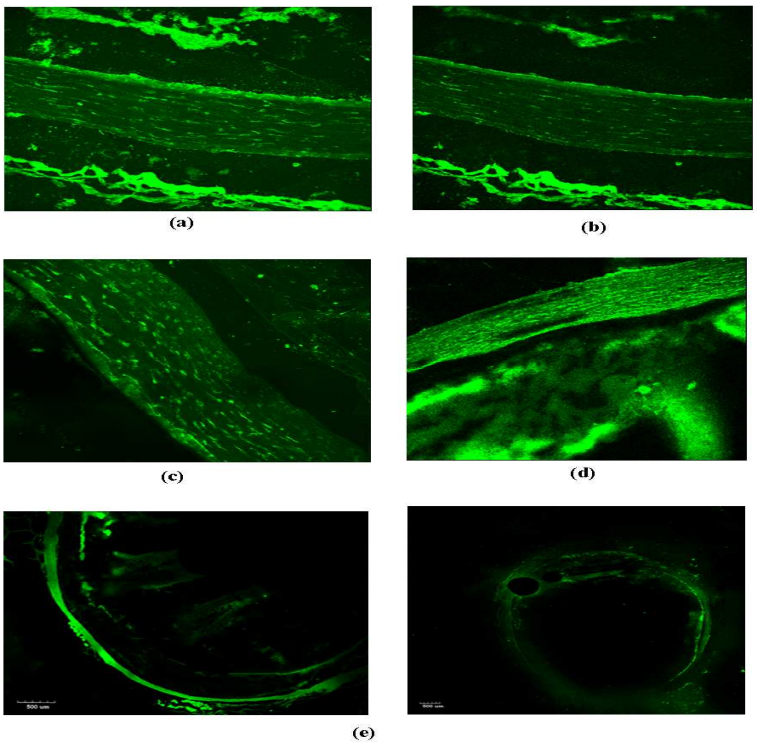

Figure 7: Fluorescent images of ocular tissues of the eye at 15 min (a), 30 min (b), 4 h (c), and 24 h (d), post F-SLN administration. Fluorescent images of cryosectioned whole ocular tissues after F-SLN administration at 30 min (e).

Confocal microscopy studies provided a direct evidence of the fact that the SLN system developed presently by us are capable of exporting the drug to ocular tissue in excess as compared to free solution which is observed in high fluorescent intensity upto 24 h in F-SLNs in comparison to F-SOL samples. Further confirmation of cellular uptake studies was also revealed in HCLE and HCJE cell lines when strong fluorescence intensity was observed for F-SLNs treated cells. Human corneal epithelial cells are the first cells

encountered by a topically instilled eye drop. If a drug can penetrate the full thickness of cornea and reach the anterior chamber in high concentration, then further diffusion into the posterior chamber should occur easily.

Transport of SLNs may occur by passive diffusion across the different compartments, although the presence of efflux transporters may also play a significant role and SLNs are known to overcome the various efflux transporters that are found in cornea.

Fluorescent microscopy (whole eye section) also provides significant evidence that SLNs reach even upto the internal eye tissue. Furthermore, the interaction of SLNs with the glycoproteins of the cornea and conjunctiva can form a precorneal depot resulting in prolonged release of the encapsulated drug. All the more, the lipidic SLNs may interact with the outer lipid layer of the tear film, increasing their residence in the conjunctival sac, where it either acts as a drug depot [26] or passively diffuses through the cornea intact. However, the stromal layer of the cornea is hydrophilic in nature. SLNs are lipidic particles dispersed in an aqueous surfactant solution, such that it depicts enhanced permeability both through the lipophilic and the hydrophilic physiological barriers.

Inspite of showing effectiveness against the pulmonary and extrapulmonary mycobacterium infections, yet no ocular formulation of INH is in the market. In ocular drug delivery the major challenges are the structure of eye in which the epithelium is the outermost structure of the cornea and is composed of six cell layers. The main characteristic of the corneal epithelium is the presence of intercellular tight junctions (zonula occludens) that prevent the diffusion of hydrophilic molecules with size >100 Da through the paracellular route. In contrast, lipophilic substances, can readily diffuse through the epithelium via a transcellular route [27].

Bioanalytical method development

System suitability

The system was found to be suitable for the determination of INH under the optimized chromatographic conditions. Average peak area per injection was determined at each time point and relative standard deviation (RSD) was ≤ 3.1% (data not shown). As per USFDA bio-analytical method validation guidelines, 2001, accuracy of the developed analytical procedure should be high and its RSD should be less than 5%.

The efficiency of the column was expressed by number of theoretical plates for the 6 replicate injections and was above 8000 and USP tailing factor was below 1.5 for all the samples. As per HPLC method of analysis of INH defined by USP the number of theoretical plates should be >2500 and tailing factor <2.0.

Specificity

High specificity of the developed method was confirmed by the absence of any interfering peaks at the retention time of INH. Further, chromatograms obtained from spiked aqueous samples were found to be specific for INH (Figure 8 c).

Sensitivity

LOD and LOQ value for INH was 400 ng/ml and 600 ng/ml respectively.

Recovery

Recovery (n = 6) for INH was found to be 96.8 ± 4.9 %, 99.5 ± 11.0 % and 99.5 ± 5.0 % for LQC, MQC, HQC samples, respectively.

Intra- day and inter-day precision and accuracy

The intra-day accuracy for INH was found to lie between 87.2–91.9 % in aqueous humor of rabbit samples with RSD less than 5% for the QC samples.

The inter-day accuracy of INH in aqueous humor rabbit samples ranged from 89.0 % to 90.3 % for the QC samples.

Table 5: Inter-day precision and accuracy of INH in aqueous humor

Nominal Concentration (ng/ml)	Observed Concentration (ng/ml)	% precision	% accuracy
Inter day			
LQC (800)	712±28.6	4.0	89.0
MQC (1200)	1084±45.0	4.2	90.3
HQC (1600)	1428±55.4	3.9	89.3

Table 6: Intra-day precision and accuracy of INH in aqueous humor

Nominal Concentration (ng/ml)	Observed Concentration (ng/ml)	% precision	% accuracy
Intra day			
LQC (800)	712.4±19.6	2.7	89.0
MQC (1200)	1103.2±17.1	1.5	91.9
HQC (1600)	1406.4±26.9	1.9	87.2

Linearity

The calibration curve for INH was found to be linear ($r^2 = 0.999$) in aqueous humor at the concentration range of 600–1600 ng/ml.

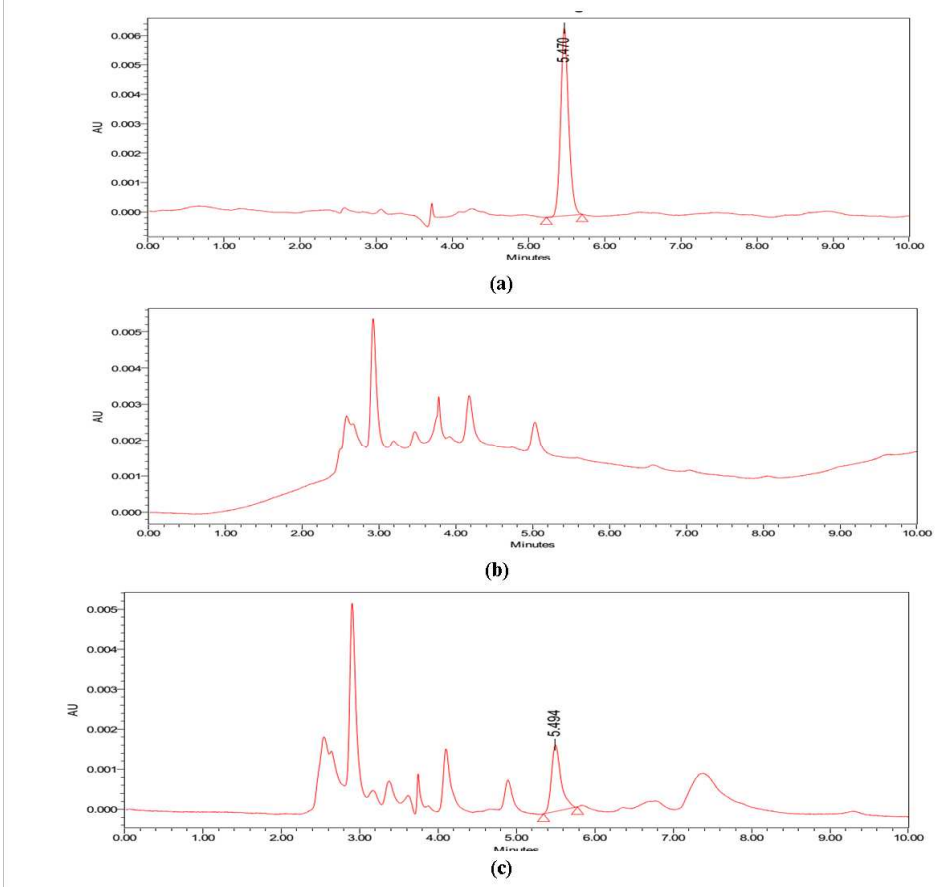

Figure 8: HPLC chromatogram of INH (a), Blank aqueous humor (b), INH in aqueous humor (c).

Pharmacokinetic parameters

The concentration-time profiles and corresponding pharmacokinetic parameters of INH-SLN and INH-SOL after topical administration into the eye were monitored and determined in the aqueous humor. A significantly ($p < 0.001$) higher C_{max} (1.5-fold) and bioavailability/AUC (427.6 % increase) for INH-SLN with respect to the INH-SOL was noted in aqueous humor. The concentration of INH in the aqueous humor in the SLN treated group was found to lie in the range of 23.31–2.10 µg/ml, over a 24 h period, which was several times higher than that observed for INH-SOL group (15.00–2.02 µg/ml at 4 h).

C_{max} of 23.31 µg/ml in aqueous humor progressively reduced to 16.37 µg/ml at 2 h followed by 12.5 µg/ml and 2.24 µg/ml at 4 and 24 h, respectively, indicating a sustained and prolonged stay of INH-SLNs in the aqueous humor as compared to INH-SOL which reduced to 2.83 µg/ml at 4 h itself (Figure 9).

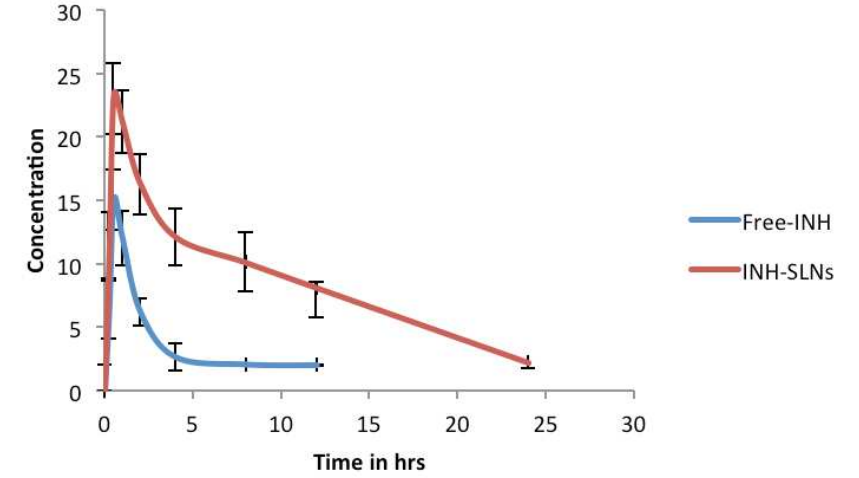

Figure 9: Comparative concentration-time profile of INH-SLNs and INH-Sol in aqueous humor following topical application to rabbit eye

Table 7: Pharmacokinetic parameters of INH-SLNs and INH-SOL following topical administration (n=6).

Formulation	C_{max}	T_{max} (h)	$T_{1/2}$ (h)	MRT (h)	AUC (µg/ml)
INH-SOL	15.09±3.10	0.25	4.69±0.17	6.19±0.37	44.00±4.62
INH-SLNs	23.31±3.10	0.25	11.00±0.82	16.04±1.12	188.13±37.10

Values are mean ± standard deviation. The results were analyzed for statistical significance by a t-test. All values observed for INH-SLNs were significantly different from those for INH-Sol, at $p < 0.001$.

Researchers have tried to deliver INH via various routes alternate to conventional route for treatment of pulmonary and extrapulmonary TB. T et al. (2015) tried to deliver the INH via transdermal route. 5% menthol, limonene or Transcutol® were evaluated by these workers as the penetration enhancers. Menthol was not able to improve the absorption of INH. Transcutol® reduced permeation flux (2.2-fold) but increased the amount of INH retained in the skin (1.7-fold). Limonene on the other hand was the most effective excipient since it increased permeation flux (1.5-fold) and lag time was greatly shortened (2.8-fold) [28]. Composite scaffold drug delivery system fabricated with an

isoniazid conjugated star poly (lactide-coglycolide) (PLGA-INH_4) and β-TCP is also reported. INH concentrations were measured in tissues around implanted sites and in blood. *In vivo* release of INH at 4, 8 and 12 weeks post-surgery was evaluated. The concentration was found higher than minimal effective treatment concentration (5-10 µg/mL) and a tissue concentration, 2-3 times higher than blood was observed [29]. We (Bhandari and Kaur, 2013) also reported a significant improvement ($p<0.001$) in relative bioavailability of INH-SLNs in plasma (6 times) and brain (4 times) after oral administration with respect to the free drug solution at the same dose.

Ocular pharmacokinetic studies, presently, show 4.27 times higher bioavailability of INH when administered as SLNs versus the free drug solution in the aqueous humor. The longer ocular retention (2.6 times MRT) in aqueous humor is due both to the small size of SLNs and presumed retention in mucopolysaccharide chains of mucin available in the precorneal area allowing extended permeation in to the aqueous humor. Another point, which is noteworthy in the study, is the fact that peak effects were obtained within (0.25 h is 15 min) min after administration of the last drop of SLNs. This indicates a fast passage of the developed system across various barriers to reach the aqueous humor. This will ensure quick control of infection.

Conclusions: Presently reported INH-SLN system can offer a local and efficient control of ocular TB without demonstrating side effects associated with the oral therapy. Highly water soluble drug was efficiently incorporated in SLNs through microemulsification and shows better corneal permeation. Corresponding safety in corneal and conjunctival cell lines followed by in vivo acute and subchronic toxicity studies in rabbits establish suitability of developed SLN formulation for ocular use. Significant uptake of fluorescein labelled SLNs in corneal and conjunctival and ocular tissues following topical administration as drops, gives the direct evidence of their efficient target ability. Improved localised concentration of INH in aqueous humor will result in effective treatment.

Reference

WHO, 2017. Global tuberculosis report, World Health Organization, Geneva pp 1-249

Dalvin LA and Smith WM, **Intraocular manifestations of mycobacterium tuberculosis: A review of the literature**. *J Clin Tuberc Other Mycobact Dis*. 2017;7:13-21

Sanches I, Carvalho A and Duarte R, **Who are the patients with extrapulmonary tuberculosis?** *Rev Port Pneumol*. 2014;21:90-93

Yeh S, Sen HN, Colyer M, Zapor M and Wroblewski K, **Update on ocular tuberculosis**. *Curr Opin Ophthalmol*. 2012;23:551-556

Shakarchi FI, **Ocular tuberculosis: current perspectives**. *Clin Ophthalmol*. 2015;9:2223–2227

Gupta V, Gupta A and Rao NA, **Intraocular tuberculosis - an update**. *Surv Ophthalmol.* 2007;52:561-587

Lopez ES, Espina M, Doktorovova S, Souto EB and García ML, **Lipid nanoparticles (SLN, NLC): Overcoming the anatomical and physiological barriers of the eye - Part I - Barriers and determining factors in ocular delivery.** *Eur J Pharm Biopharm*. 2017:70-75

WHO, 2003. *Treatment of tuberculosis*, World health organization, Geneva.

Metushi IG, Cai P, Zhu X, Nakagawa T and Uetrecht JP, **A fresh look at the mechanism of isoniazid-induced hepatotoxicity**. *Clin Pharmacol Ther*. 2011;89:911-914

Bhandari R and Kaur IP, **Pharmacokinetics, tissue distribution and relative bioavailability of isoniazid-solid lipid nanoparticles.** *Int J Pharm*. 2013;44:202-212

Kaur IP and Bhandhari R, **Solid lipid nanoparticles entrapping hydrophilic/amphiphilic drug and a process for preparing the same, WO 2013105101 A1**. 2013

Aggarwal D, Garg A and Kaur IP, **Development of a topical niosomal preparation of acetazolamide: preparation and evaluation**. *J Pharm Pharmacol*. 2004;56:1509-1517

Kakkar S, Karuppayil SM, Raut JS, et al., **Lipid-polyethylene glycol based nano-ocular formulation of ketoconazole**. *Int J Pharm*. 2015;495:276-289

Hassan A, Fattouh M, Atteya I, Mohammadeen H and Ahmed H, **Validation of A rapid tuberculosis PCR assay for detection of MDR-TB patients in sohag University Hospital**. *Appl Environ Microbiol.* 2014;2:65–69

Gupta R, Thakur B, Singh P, et al., **Anti-tuberculosis activity of selected medicinal plants against multi-drug resistant *Mycobacterium tuberculosis* isolates**. *Indian J Med Res*. 2010;13:809-813

ICH, 2005. *Harmonised tripartite guideline validation of analytical procedures: text and methodology*.

Kumar M, Kakkar V, Mishra AK, Chuttani K and Kaur IP, **Intranasal delivery of streptomycin sulfate (STRS) loaded solid lipid nanoparticles to brain and blood**. *Int J Pharm*. 2014;461:223-233

Sinclair GW and Peppas NA, **Analysis of non-fickian transport in polymers using simplified exponential expressions**. *J Memb Sci.* 1984;17:329-331

Malhotra M and Majumdar DK, **Permeation through cornea**. *Indian J Exp Biol*. 2001;39:11-24

Sieg JW and Robinson JR, **Mechanistic studies on transcorneal permeation of pilocarpine**. *J Pharm Sci*. 1976;65:1816–1822

Kreuter J, **Nanoparticulate systems for brain delivery of drugs**. *Adv Drug Deliv Rev*. 2001;47:65-81

Wasan KM, **Formulation and physiological and biopharmaceutical issues in the development of oral based lipid-based drug delivery systems.** *Drug Dev Ind Pharm*. 2001;27:267–276

Dumas F and Haanappel E, **Lipids in infectious diseases - The case of AIDS and tuberculosis.** *Biochim Biophys Acta*. 2017;1859:1636-1647

Pandey AK and Sassetti CM, **Mycobacterial persistence requires the utilization of host cholesterol**. *Proc Natl Acad Sci U S A*. 2008;105:4376-4380

Kaur IP and Singh H, **Nanostructured drug delivery for better management of tuberculosis**. *J Control Release*. 2014;184:36-50

Urtti A, **Challenges and obstacles of ocular pharmacokinetics and drug delivery**. *Adv Drug Deliv Rev* 2006;58:1131-1135

Trabado JA, Diebold Y and Sanchez A, **Designing lipid nanoparticles for topical ocular drug delivery**. *Int J Pharm*. 2017;532:204-217

Caon T, Campos CE, Simoes CM and Silva MA, **Novel perspectives in the tuberculosis treatment: Administration of isoniazid through the skin**. *Int J Pharm*. 2015;494:463-470

Huang D, Li D, Wang T, et al., **Isoniazid conjugated poly(lactide-co-glycolide): long-term controlled drug release and tissue regeneration for bone tuberculosis therapy.** *Biomaterials*. 2015;52:417-425

Supplementary Data

Development of isoniazid loaded solid lipid nanoparticles for ocular delivery with proof of concept: *In vitro* characterization, antimycobacterial, pharmacokinetics and safety evaluation.

Mandeep Singh, Ana Isabel Guzman Aranguez, Afzal Hussain, Cheerneni Sai Srinivas,

Indu Pal Kaur

Characterisation of INH-SLNs

Developed INH-SLNs were characterised exhaustively for TDC, EE, particle size and zeta potential. Morphological characterization was done using AFM and TEM, followed by DSC, FTIR and NMR

Total drug content (TDC) and entrapment efficiency (EE)

SLN dispersion (0.1 ml) was treated with 5 ml mixture of chloroform: methanol (3:1) and diluted with water upto 10 ml in 15 ml centrifuge tube. The tube was shaken to mix the contents and centrifuged at 9000 rpm for separation of water and chloroform layer. The water layer was collected and diluted suitably to measure the total drug content by HPLC. Chloroform helps to dissolve the lipid matrix and disrupt the formed SLNs.

EE was determined by adding 1M magnesium sulphate to INH-SLN dispersion (1 ml) in eppendorf tube followed by vortexing. The dispersion was then centrifuged at 15000 rpm for 15 min to separate the flocculated SLNs from free drug in the supernatant. INH was determined by HPLC in both the pellet (entrapped drug) and the supernatant (unentrapped/ free drug).

Particle size and zeta potential

Mean diameter of SLNs in the dispersion (10X dilution) was determined using photon correlation spectroscopy at an angle of 15, 30 and 160 degree having laser diodes 658 nm as light source and zeta potential was determined by forward scattering through transparent electron technology using flow cell assembly (Beckman Coulter, Delsa nano C).

Atomic force microscopy

Atomic force microscopy studies were performed using AFM apparatus (JPK Instruments, Germany). An Intermittent contact mode (ICM) in air atmosphere, at the ambient pressure (about 760 mm of Hg) and temperature (20 ºC) was used to reduce the deformation of the sample that occurs while scanning in contact mode. A 20 µl droplet of INH-SLN sample, diluted 200X times in water, was used to deposit on silicon surface. All the measurements were performed immediately after the water evaporation. A rectangular AR5-NCLR (NANOSENSORS) silicon n-cantilevers, ~165 kHz and ~48 N/m, with a nominal tip radius less than 15 nm, were used. AFM

defines the surface morphology of particles by means of the topography and ICM phase data. All AFM images were analysed using JPK data processing software.

Morphological evaluation using transmission electron microscopy (TEM)

For observation under TEM, INH-SLNs after suitable dilution (20X) with distilled water were stained with 2% phosphotungstic acid (PTA) in phosphate buffer (pH 6.8) for 5 min, after which the excess PTA was removed. Sample was spread on a carbon coated copper grid which was then observed under TEM (FE Teenai G2 F20, Netherlands) at a voltage of 120 kV, for morphological parameters like size, sphericity and aggregation.

FTIR

FTIR spectra of Combi lipid (1:4 combination of stearic acid and Compritol 888 ATO®), INH, Blank SLNs (SLNs prepared without drug), and INH-SLNs were recorded using KBr pellet technique on an IR spectrophotometer (Perkin Elmer, USA).

Powder X-ray diffraction (PXRD)

The crystalline/amorphous nature of INH-SLNs was confirmed by X-ray diffraction measurements using X-ray diffractometer (XPERT-PRO, PANalytical). PXRD studies on INH and lyophilised Blank SLNs and INH-SLNs were performed by exposing the samples to CuKα radiation (45 kV, 40 mA) and scanning from 5º to 50º, 2θ at a step size of 0.017º and scan step time of 25 second. Obtained PXRD patterns were compared with the characteristic drug peak intensity obtained from INH.

Differential scanning calorimetry (DSC)

DSC thermograms of Combi-lipid, INH, INH-SLNs and blank SLNs were recorded on Q20 Differential Scanning Calorimeter. Weighed quantity (2 mg) of each component was added to aluminium pans and heated at predetermined rate of 10 ºC/min over the temperature range of 30 to 300 ◦C in presence of nitrogen. Thermal data analysis of thermograms was conducted using TA instruments universal analysis 2000 software. The recorded scans were plotted between heat flow (W/g) and temperature. The calibration of calorimeter was performed using Indium as a standard.

Nuclear magnetic resonance (NMR) spectroscopy

^{1}H NMR spectra were recorded by an Avance II 400 spectrometer (Bruker, Rheinstatten, Germany), operating at 400MHZ. Aliquots of INH, Blank-SLNs, and INH-SLN dispersion was filled in NMR tube. Accurate quantity of deuterated water was added for field login and tetramethylsilane (TMS) was added as reference for 0 ppm.

Safety of INH-SLNs

A two tier *invitro* toxicity dermal toxicity (preamble to ocular toxicity) and/acute ocular toxicity evaluation of INH-SLNs were done in rabbits as per OECD. Further repeat dose (5 times) and chronic repeat dose (one week) study was also conducted in rabbits as per previously reported procedure [1]. Details of these studies are included in the supplementary data. Any adverse effects of INH-SLNs on ocular tissue was also confirmed under the ocular tolerance study.

Cytotoxicity studies

The viability of stratified HCLE (human corneal - limbal epithelial), and HCJE (human conjunctival epithelial) cell lines exposed to INH-SLNs was determined by a cell proliferation assay using MTT (3-(4,5-Dimethyl-2-thiazolyl)-2,5-diphenyl-2H-tetrazolium bromide). Cells grown in keratinocyte serum-free medium (Invitrogen, Carlsbad, CA) and supplemented with 25 µg/ml bovine pituitary extract, 0.4 mM $CaCl_2$, 0.2 ng /mL epidermal growth factor (EGF) and suitable antibiotics were maintained at 37 ºC in 5% CO_2. For efficient stratification and differentiation, upon reaching confluence, the culture medium was replaced with Dulbecco's minimal essential medium (DMEM)/F12 medium supplemented with 10% calf serum and 10 ng/ml EGF for 7 days [2].

Stratified HCLE and HCJE cells in DMEM/F12 medium were exposed for 24 h to various samples viz. INH-SOL, Blank-SLNs and INH-SLNs at a concentration of 1µg/ml and 10 µg/ml. After exposure, MTT test was used to assess cellular viability as described previously [3]. Briefly, fresh MTT solution (0.5 mg/ml) was added to cells, which were then incubated for 2 h at 37 ºC. Following incubation, cells were lysed and the released purple formazan was dissolved in dimethyl sulfoxide.

Absorbance of the samples was read using Gen 5 plate reader (BioTek, Winooski, VT, USA) at 570 nm and corrected for background by subtracting the absorbance at 690 nm from that at 570 nm. The mean absorbance values of non-treated cells were taken as 100% and results are expressed as percentage cell viability compared to the control (non-treated) cells. Experiments were performed in triplicate.

Dermal irritation/corrosion test as per OECD guideline 404 (ADI, 2002)

This test was conducted to confirm the safety of the formulation for dermal application. According to OECD guideline 405, the in vivo eye irritation/corrosion test, should preferably be preceded by a study establishing the in vivo dermal safety (OECD testing guideline 404) as a preamble to ocular toxicity studies [4].

Young female albino rabbits of age around 6 months (weight of 1.3-1.7 kg) with intact skin were used in the study. Fur was removed from the dorsal trunk area of the test animal using hair clippers followed by the application of a hair removing cream, 1 day before the test. INH-SLNs (0.5 ml) applied uniformly onto a 6 cm^2 gauze patch were applied to the cleared skin and fixed with non-irritating tape. First patch was removed after 3 min, and if no reaction was observed then a second patch was applied for 1 h. In case of the absence of any reaction the study was extended for a period of 4 h. Good contact of the test formulation with the skin was ensured. Application site was so selected that the access of the animal to the patch was limited so that ingestion of the patch was not possible. Some shaved skin area near the test area was reserved as control. At the end of the test, the gauze patch was removed, and the skin was examined 4 h after patch removal, for signs of erythema and redness as described previously [1]. The test was performed first on a single animal and its response graded. Once the test on first animal showed absence of irritation/corrosion, the negative response was confirmed using two additional animals.

Eye irritation/corrosion test as per OECD guideline 405 (AEI, 2002)

INH-SLN dispersion (0.1 ml) was instilled in the conjunctival sac of the right eye of each rabbit (n=3) once and also five times at regular (5 min) intervals (for repeat test) by gently pulling the lower lid to create space for instillation. Left eye served as a control in each case. The eyes were examined regularly at 1, 24, 48, and 72 h after application of the test drops and scored as per the scale described in the OECD guidelines [1, 5]. A chronic repeat dose study in which the test formulation was

instilled five times (at 5 min interval) every day in the conjunctival sac of rabbits, for a period of one week, was performed to establish the safety for long term therapy [1].

Ocular tolerance evaluation

To examine the effects of INH-SLNs on ocular structure and integrity, the left eyeball was removed from rat eyes 0.5 h, 1 h and 2 h post administration of SLNs to the left eye of the rat. Right eye of these animals was taken as control. The eye balls were washed with saline and fixed with 8% v/v formalin solution. The material was dehydrated with an alcohol gradient, put in melted paraffin and solidified in block form. Cross-sections (<5 μm) were cut, stained with haematoxyline and eosine (H and E) and microscopically observed (Nikon eclipse 90i, Japan) for any pathological effects.

Result and Discussion

Total drug content (TDC) and entrapment efficiency (EE)

The drug content of the developed INH-SLNs was 14.50±0.54 mg/ml which was 91.6±3.4% of what was originally incorporated (16 mg/ml) and the EE was 65.2±2.2% (n=6).

Note: Previously prepared INH-SLNs by our group [6] were loaded with 10% INH with respect to the lipid matrix, though it showed higher EE of > 80%.

Particle size and zeta potential

The developed INH-SLNs showed an average particle size (n=6) of 149.2 ±4.9 nm and PDI of 0.15±0.02 (n=6) (Figure S1). The zeta potential was found to be -0.35 ± 0.28 mV (Figure S2).

Liposomes with a size of 105–125 nm were found to reach the retina whereas the corresponding micrometer size liposomes did not show significant penetration [7]. Nano-sized particles are also reported to show better bioadhesion [8] and greater surface for association with the cornea and conjunctiva. They can also pass across the anatomical constraints of the eye and provide enhanced penetration through the cornea[9, 10]. Nanoemulsions interact with the lipid layer of the tear film, remaining in the conjunctival sac for longer times, and consequently acting as a drug depot [11]. Similarly, the nanoparticulate nature of SLNs will also impart an increased residence time on the ocular surface in turn enhancing permeability and hence ocular bioavailability. An increase in particle size from 48.4 nm reported previously (Bhandari and Kaur 2013) to the present value of 149.2 nm is attributed to 4 times increase loading of INH (from 10% to 40%) presently. An increase in size with increase in loading of drug is also reported elsewhere [12].

The near neutral zeta of SLN dispersion guarantees a physical stability of the colloidal dispersion. As per the DLVO (named after inventors Derjaguin, Landau, Verwey and Overbeek) theory, the colloid stability depends on the sum of Van der Waals attractive forces and electrostatic repulsive forces due to the electron double layer [13]. While zeta potential provides information on the electrostatic repulsive forces it does not provide any insight on the attractive Van der Waals forces. Therefore, it is not uncommon to come across stable colloids with low zeta and vice versa. The same is reported by us earlier also for the preparation of rifampicin SLNs

(−3.5 ± 0.80), ethambutol SLNs (-5.6± 0.90) and ketoconazole SLNs (3.19) in our lab [1, 14].

Tween 80 used presently as an emulsifier for production of INH-SLNs is non-ionic in nature. It is however indicated that non-ionic surfactants assign a negatively charged interface at neutral pH as seen presently. This was attributed to differential absorption of hydroxyl and hydronium ions on the interface [15].

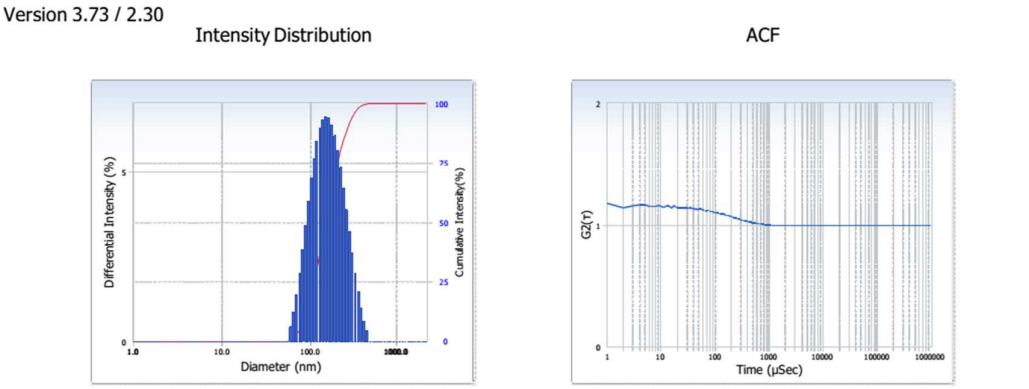

Distribution Results (Contin)

Peak	Diameter (nm)	Std. Dev.
1	178.2	77.8
2	0.0	0.0
3	0.0	0.0
4	0.0	0.0
5	0.0	0.0
Average	178.2	77.8
Residual :	3.206e-003	(O.K)

Cumulants Results

Diameter	(d)	: 148.7	(nm)
Polydispersity Index	(P.I.)	: 0.160	
Diffusion Const.	(D)	: 3.412e-008	(cm²/sec)

Measurement Condition

Temperature	: 26.2	(°C)
Diluent Name	: WATER	
Refractive Index	: 1.3327	
Viscosity	: 0.8641	(cP)
Scattering Intensity	: 27078	(cps)
Attenuator 1	: 14.07	(%)

Figure S1: Particle size distribution of a representative INH-SLNs batch

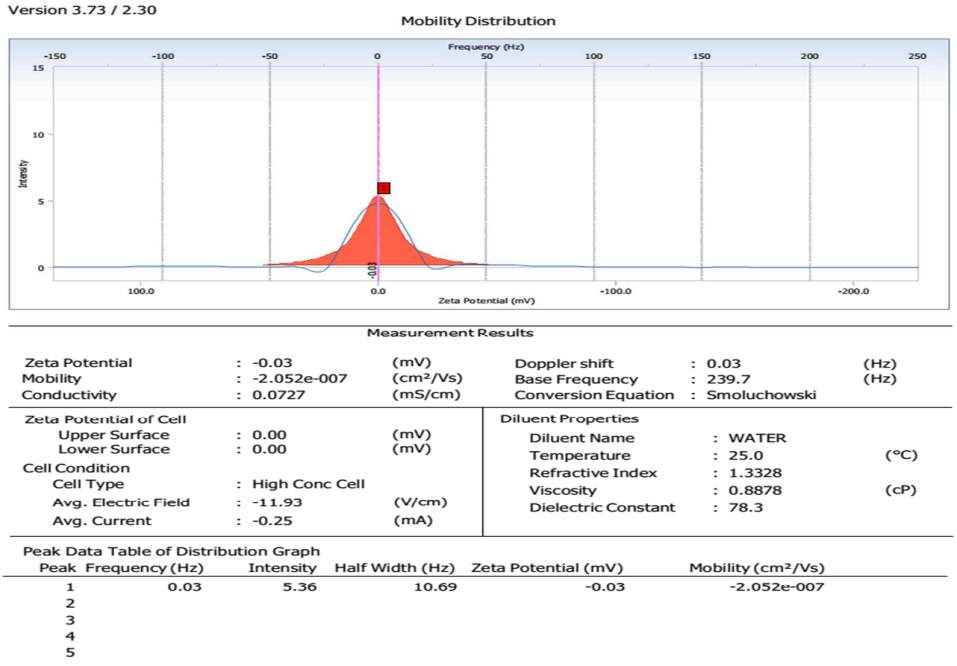

Figure S2: Zeta Potential of one batch of INH-SLNs

Particle size and zeta potential in biological fluids

The average particle size and PDI of developed INH-SLNs in simulated tear fluid (STF; pH 7.2) [16] increased to almost a double size (316.5±8.7 nm) with PDI, 0.24±0.22. The size also increased significantly to 231.4±5.3 nm with PDI 0.35±0.01 at pH 7.4 in PBS.

The zeta potential however did not change significantly ($P \leq 0.15$) both in STF (+0.24±0.2 mV) and PBS at pH 7.4 (-0.11±0.04 mV).

The significant increase in particle size in STF and at pH 7.4 is due to the presence of electrolyte salts in these fluids. The smallest particle size and narrow size distribution was achieved in electrolyte free aqueous SLN suspension [15]. Presence of electrolytes trigger destabilisation of SLN dispersion by reducing the electrostatic repulsive force between the particles resulting in their coalescence to form bigger particles [17]. It is also indicated that near zero charge (as is the case presently; zeta potential of aqueous INH-SLNs dispersion is -0.35 mV) dispersion coalescence more easily [18].

Atomic force microscopy (AFM)

Topographic AFM images of formulated SLNs showed a diameter of 800 nm, and a height of 75 nm (Figure S3).

Size was larger than that observed by PCS technique and TEM. It may be due to sample preparation for AFM, when bulk water molecules although removed by evaporation at 25 ºC over a 24 h can result in practically hydrated SLNs which show a size larger than their actual size. 3D cross-section images (Figure S3) confirm a matrix structure for the SLNs, mechanically resistant to collapse. Nevertheless, a flattening of SLNs by probe impact may account not only for a reduced height but also increase in the diameter of the SLNs due to a probe flattening effect [19].

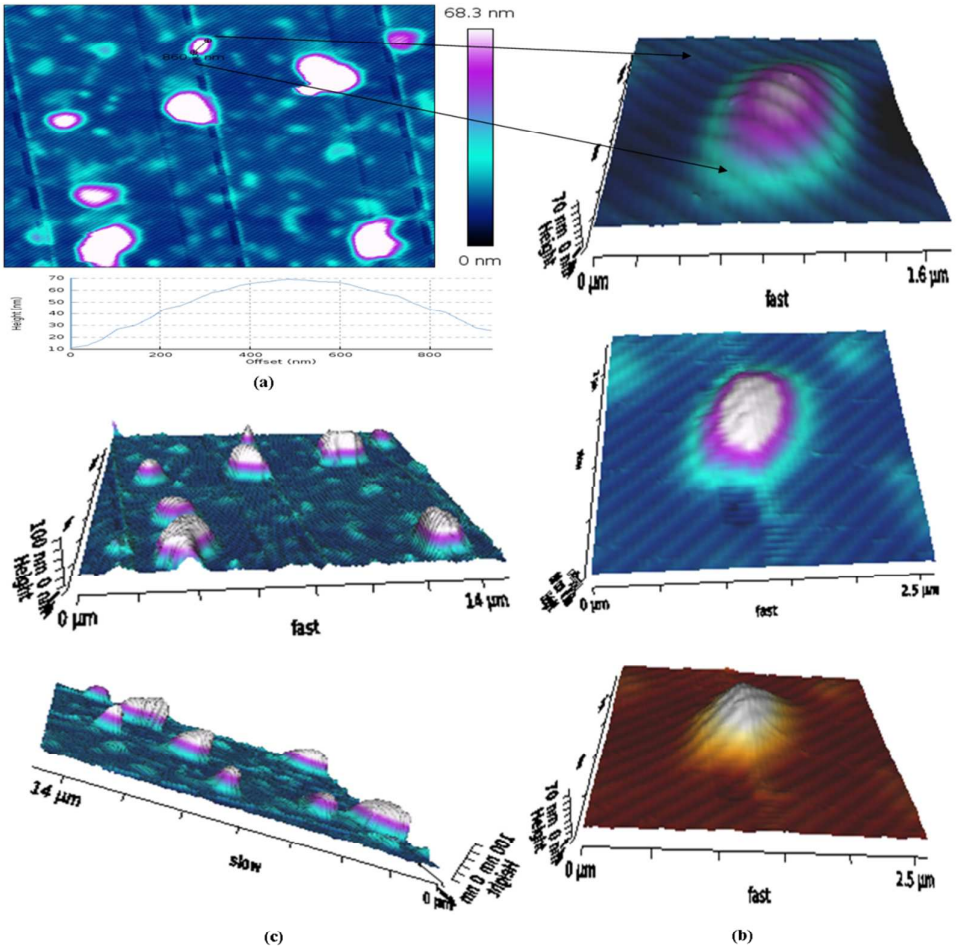

Figure S3: Atomic force microscope images of a INH-SLNs (a) topographic image (vertical status-bars are representing the height data); (b) and (c) pseudo-3D topographic images of a single particle at different angles.

Transmission electron microscopy

Morphological analysis of INH-SLN in aqueous dispersions, detected by TEM analysis, indicate polyhedral to spherical particles varying from 63 - 117 nm (Figure S4) in size. Average particle size obtained with dynamic light scattering (DLS) was 149.2 nm; DLS measures hydrodynamic diameter which is usually more than the actual particle size [20].

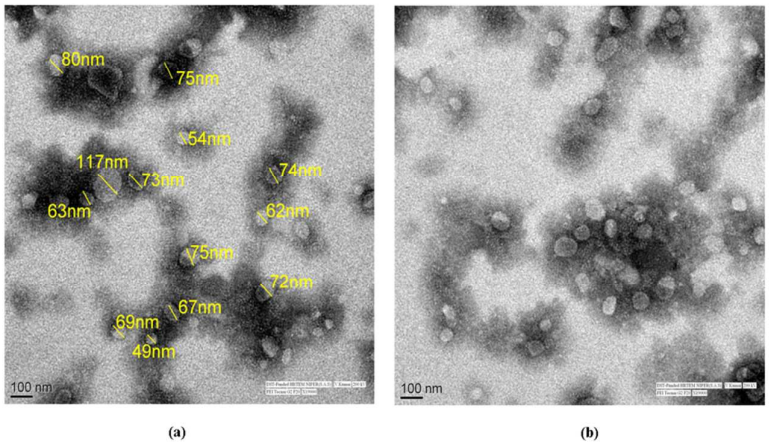

Figure S4: HRTEM images of INH-SLNs 19000X (a) and (b) at 200kv

Particle shape is a crucial parameter, exerting significant impact on cellular uptake, uptake kinetics and mechanism, intracellular distribution and cytotoxicity of nanoparticles. The order of cellular uptake of nanoparticles is reported as sphere >cube > rod > disk, probably due to ease of bending of cell membrane around the particles. The study revealed that the, spherical shape seems more favourable to improve the efficacy of the cargo [21].

The polymorphic form of SLNs also reflects in the shape of the particles; particles in α modification form are usually observed circular to polyhedral [22].

FTIR studies

The FTIR spectrum of pure isoniazid exhibited characteristic peaks of carbonyl C= O bond (1666 cm^{-1}), amino group NH_2 (1331 cm^{-1}), N-N single bond (1219 cm^{-1}), N-H

bending (1554 cm^{-1}), C-H bond of the aromatic ring (3015 cm^{-1}), and C-C=O bending (671 cm^{-1}). Combi lipid exhibited characteristic peaks at 2919 cm^{-1} and 2850 cm^{-1} (alkanes stretch) and 1741 cm^{-1} (C=O ester stretch). Blank-SLNs also exhibited the same characteristic peaks but with reduced intensity as compared to the pure lipid. However, there is a change in the CH assymetric stretch from 2850 for the lipid combination to 2857 cm^{-1} in both blank and INH-SLNs (Figure S5).

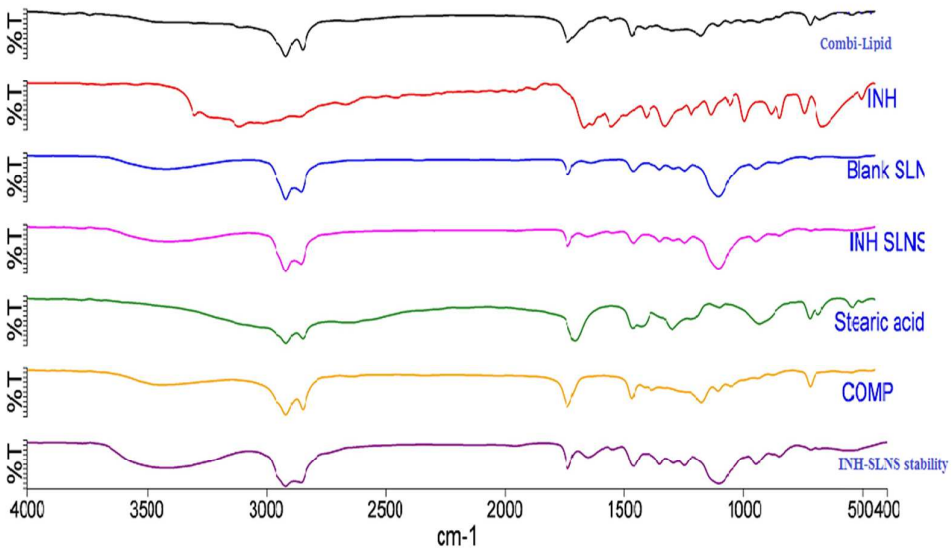

Figure S5: FTIR spectra of Combi-lipid, INH, Blank-SLNs, INH-SLNs, Stearic acid, Compritol®888 ATO (COMP) and the INH SLNs stored at 2-8 ºC for 6 months (INH-SLN stability).

In SLNs, the vibrational modes due to functional groups particularly, the stretching oscillations provide information about the conformation (Trans gauche) dynamics and type of crystallographic subcell. The lipid polymorphs of crystalline or quasi crystalline structures display the lateral packing which is characterized as highly ordered all trans-confirmation of the polymethylene chain. The hydrocarbon chain-melting phase transitions are accompanied by the broadening of all IR-active bands and by an overall decrease in their amplitudes as observed presently for the Blank and INH-SLN spectra with respect to bulk lipid. The methylene symmetric stretching ($svCH_2$) and methylene antisymmetric stretching ($asvCH_2$) vibrations give rise to IR-active bands centred near 2850 cm^{-1} and 2919.27 cm^{-1}, respectively as seen with Combi lipid. The conformational disordering of an all-trans polymethylene chain is accompanied by an upward shift in the $svCH_2$ IR band maxima by almost 7 cm^{-1} as is observed for the IR spectra of both Blank and INH-SLNs. This reflects a probable hydrocarbon chain conformational disorder.

Although the 2920 and 2850 cm^{-1} IR absorption bands can both be used to monitor hydrocarbon phase transitions, but the 2920 cm^{-1} band is rarely used in practice. This is because the asvCH_2 band contains significant overlapping contributions from CH_3 groups and is even perturbed by Fermi resonance interactions with the first overtones of the CH_2 scissoring vibration [23, 24]. The IR band at 2850 cm^{-1} is usually not perturbed by these factors and under most circumstances arises predominantly from the symmetric C-H stretch of the CH_2 group. SLN formulations are hallmarks of a collective trans-gauche isomerization of the glyceride alkyl chains. This alteration in lipid conformation will lead to lattice imperfections as observed by the qualitative upward shifts of the peak contours detected for the C-H bands at 2857 cm^{-1}. Former would allow better and greater entry or encapsulation of drug in the free space generated between the disrupted fatty acid chains. The INH-SLNs show an almost similar spectrum even after storage for 6 months under refrigerated conditions, confirming absence of any phase inversion in the samples (Figure S5). Latter is the most important concern with SLN formulations [25].

XRD studies

Powder X-ray diffraction study of pristine drug (INH), Combi lipid, lyophilized Blank-SLNs and INH-SLNs was performed to confirm the amorphous or crystalline nature of SLNs (Figure S6). INH showed peaks at 2θ value of 11.9, 15.5, 16.5, 19.5, 23.8, 25.0 and 40.2. Combi-lipid showed sharp peaks at 2θ value of 21.2 and 23.3. Blank SLNs however did not show any peak corresponding to these values except small peaks at 2θ scattering angle of 4.8. INH-SLNs did show some peaks at 2θ scattering angle of 15.9, 19.4 and 23.7 (may be due to the un-entrapped/ free drug ~35 % in the INH-SLN dispersion. Free drug was not removed from the SLN formulation). The peak intensities of SLNs were however weak, small and diffuse indicating an amorphous or at the most only a partially recrystallized lattice. The stability sample of INH-SLN (6 month) did not show any difference from the fresh INH-SLN sample.

The chance for efficient incorporation of drug is known to decrease with increasing crystal lattice and polymorphic transition to a stable β' or β form, which can result in sustained expulsion of the drug upon storage. However since the XRD pattern of the stability samples of INH-SLN is equally diffuse with no observable, new crystalline peaks it may be concluded that the drug is not expulsed from the SLNs during storage (Figure S7). Latter is also confirmed by no significant change in the value of EE of stored INH-SLN samples (Table 1).

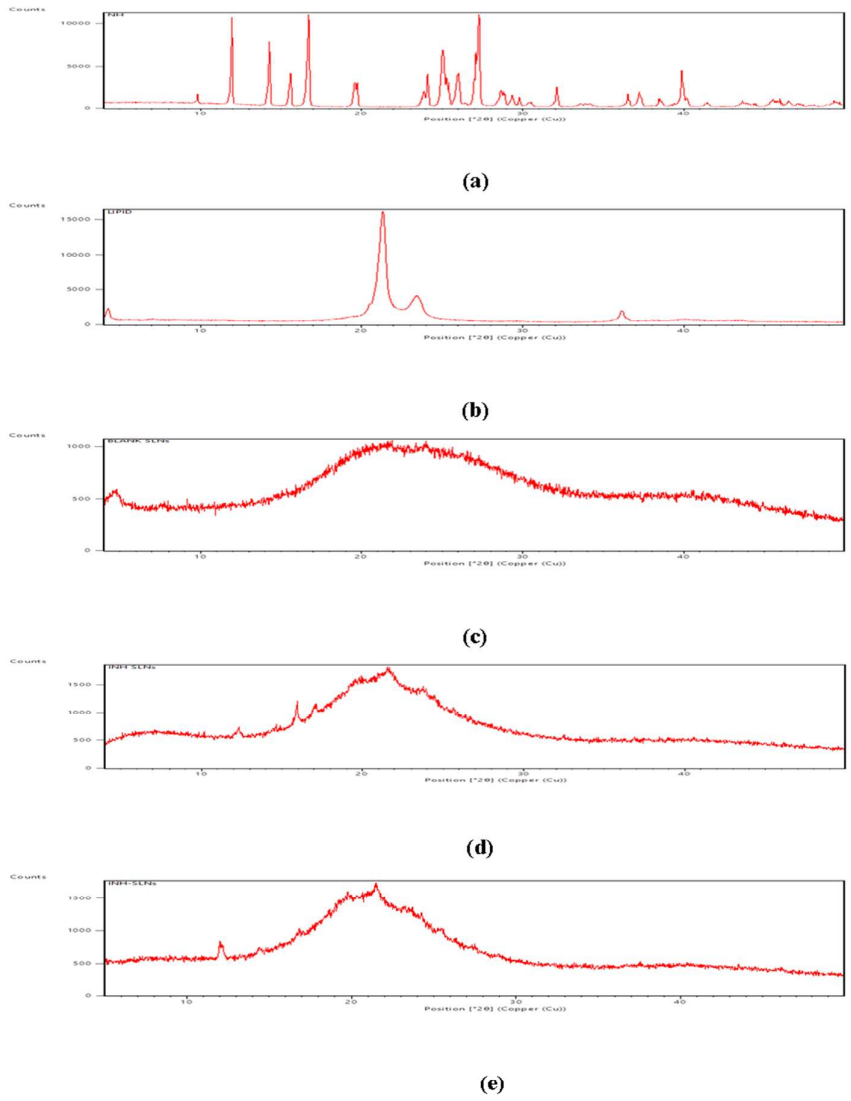

Figure S6: Powder X-ray diffraction patterns of INH (a), Combi-lipid (b), Blank-SLNs (c), INH-SLNs (d), INH-SLNs (Stability sample) (e).

Differential scanning calorimetry (DSC) of SLNs

The DSC profiles of the developed formulation and bulk lipid often show their thermal behaviour which is influenced by their crystallinity. The heating (or melting) of lipid and cooling (or recrystallization) of the hot lipid emulsion to form SLNs can lead to changes in the crystallinity and polymorphic form of a lipid. DSC is a

characterization technique which was performed presently to investigate the crystallinity of lipid in SLNs. The DSC profile of bulk Combi lipid (a combination of Compritol 888 ATO® and Stearic acid) shows a sharp melting transition at 73.67 ºC, also represented as T_{max} in Table S1.

Table S1: Differential scanning calorimetry (DSC) data of SLNs

Sample	T_{onset} (ºC)	T_{max} (ºC)	ΔH (J/g)
Combi-Lipid	**72.22**	**73.67**	**55.50 J/g**
Blank SLNs	**71.33**	**76.76**	**64.67 J/g**
INH-SLNs	**70.74**	**71.53**	**0.46 J/g**
Stability sample	**69.38**	**72.01**	**15.47 J/g**

Thermal behaviour of Blank-SLNs and INH-SLNs is shown in (Figure S7). INH-SLNs show a melting endotherm at 71.53 ºC corresponding to the Combi lipid at 73.67 ºC, whereas Blank SLNs show an upstream shift of the endotherm to 76.76 ºC but with broad peak intensity. Latter indicates the amorphousness of a less ordered crystal structure. The reduction in crystallinity would imply opportunity for successful incorporation of drug in the lipid matrix. The lower T_{max} of INH loaded SLNs with a significantly lower enthalpy as compared to both bulk Combi-lipid and Blank SLNS indicate high incorporation of drug into the SLNs. Incorporation of a drug into the lipid matrix increases the imperfections in crystal of lipid with more imperfections requires less energy which leads to decrease in melting enthalpy of the SLNs. Since size of the SLNs was < 200 nm, hence an energetically suboptimal state is created due the high surface energy associated with nanoparticles. This causes a reduction in the melting point of the lipid (as observed for INH-SLNs) due to the "Gibbs-Thomson" or "small size" effect [25-28]. It is also implied, that the reduction of particle size and crystallinity, leads to 'missing neighbours of the crystalline arrangement' that lead to weaker Van der Waals interactions and thus to a reduced Gibbs free energy of the lattice that results in a drop in the melting temperature with decreasing particle size. The lipidic nanoparticles are usually more or less polydisperse thus the melting transition is not only shifted to lower temperatures but is also broadened since the fractions of different particle sizes melt at different temperatures. Similar behaviour of lower melt temperature and enthalpy continues to be observed in thermogram of the INH-SLNs stored for 6 months (stability sample).

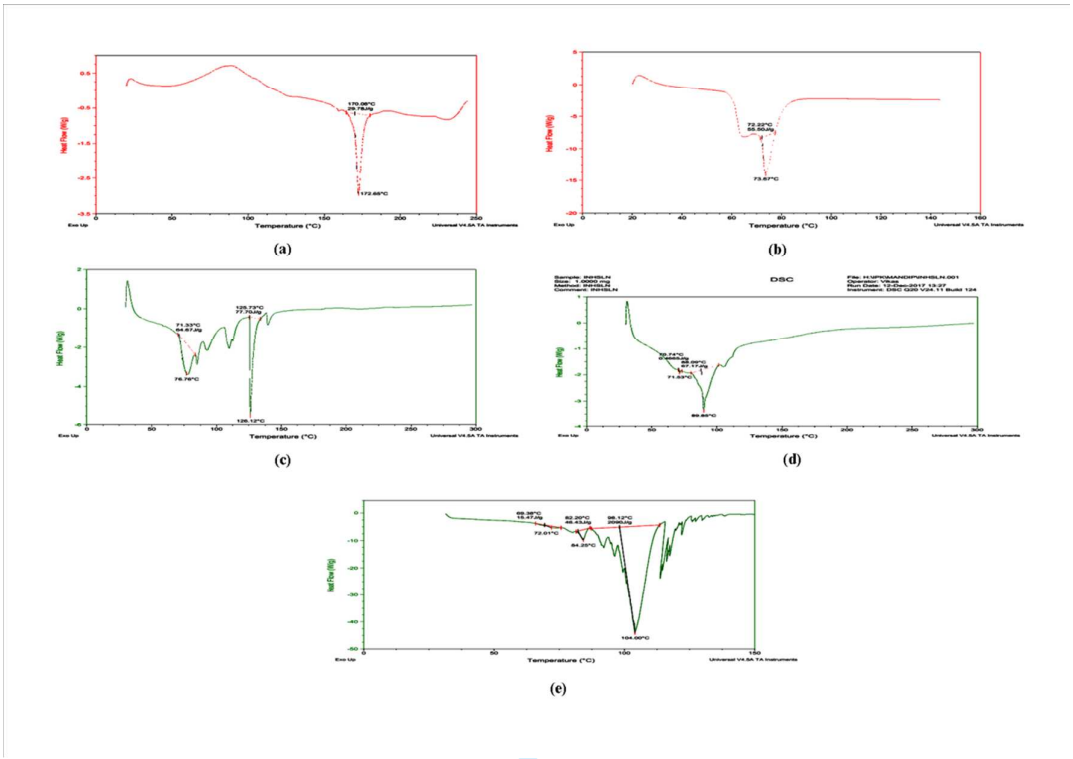

Figure S7: Thermogram of INH (a), Combi-lipid (b), Blank-SLNs (c), INH-SLNs (d), INH-SLNs (stability).

^{1}H NMR Studies

Following NMR spectra were obtained for various components of INH-SLNs and the Blank and INH-SLN formulations:

INH - (400MHz, D_2O) δ 7.4 (2.0H, s), 8.4 (2H, s)

Combi Lipid - (400MHz, $CDCl_3$) δ 0.8 (3H, m), 1.6 (31H, s), 2.2 (2H, d)

Phospholipon® ^{1}H - (400MHz, D_2O) δ 2.1, 3.1 (4H, d), 3.5 (2H, d), 3.6 (1.7H, s), 3.7 (1H, d)

Tween 80 - (400MHz, D_2O) δ 0.8(0.73, s), 1.2(18H, s), 1.2(3H, s), 1.8 (4H, s), 2.2(3H, s), 3.5(70H, s).

Blank-SLNs - (400MHz, D_2O) δ 0.5 (0.2 H, d) δ 0.9 (1H, d), 3.3 (4H, s)

INH-SLNs - (400MHz, D_2O) δ 0.7 (6H, d), δ 1.1(35H, d), δ 1.4 (3.6H, s), δ 1.8 (5.5, s), δ 2.1 (3.7 H, s), δ 3.5 (125H, s), δ 7.5 (2.0H, d), δ 8.5(2.0H, d).

^{1}H NMR spectra of INH, Combi lipid, Phospholipon® 90H (Soya 90H), Tween 80, Blank-SLNs and INH-SLNs are shown in (Figure S8). ^{1}H NMR can be used

efficiently to gain information on the molecular mobility and on material viscosity consequently. In the extreme limit for a completely solidified matrix, peak broadening or no signal (non-mobility) is expected to appear in the spectra recorded under aqueous dispersion of SLNs.

The main resonance regions observed in SLNs is as follows: (i) 0.7–2.1 ppm range, reflecting the methyl protons of the saturated aliphatic chains; (ii) 3.0–5.0 ppm range attributed to the protons of CH, CH_2, CH_3 groups belonging to glycerol, ethylene glycol (PEG) and choline/ethanolamine moieties; and (iii) 5.0–6.0 ppm region, for which signals of methine protons owing to trigliceridyl moiety and unsaturated fatty acid chains are detected. The signal corresponding to Tween 80 at 3.5 ppm appears as a specific singlet in both blank and INH-SLNs (3.3 ppm for blank SLNs, 3.5 for INH-SLNs) indicating its presence in the SLN shell. The INH signals are detected at 7.4 ppm and 8.4 ppm and were fairly seperate. The signals of INH in INH-SLNs (δ 7.5 ppm and δ 8.5 ppm) were observed. This may either be due to higher drug payload which is present in the shell, [29] or due to unentrapped INH (35 %). The INH signal in SLN showed lower amplitude with broader lines, which could be attributed to the strong interaction between the INH molecule and the lipid indicating restricted mobility of INH in SLNs [30]. The broad resonance signals in 0.7–2.1 ppm range in INH-SLNs indicates highly restricted mobility of the acylglycerol molecule of lipid as compared to the sharp signals obtained for the Combi lipid.

The Phospholipon® 90H peak at 2.1 ppm however either disappeared in Blank or showed a weak signal in INH-SLNs indicating its incorporation between the Tween 80 outer layer and the lipid core of SLNs.

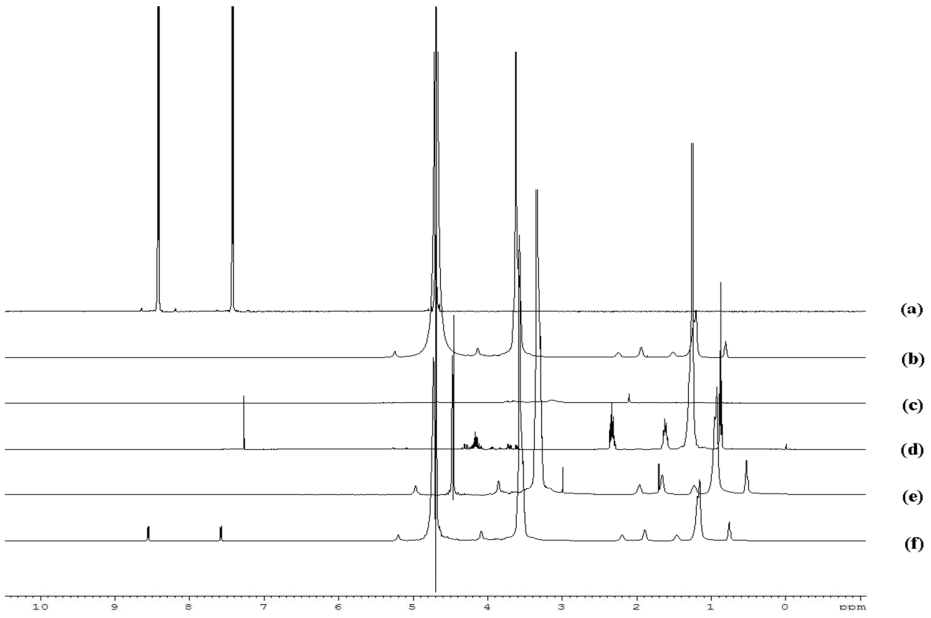

Figure S8: NMR spectra of INH (a), Tween 80 (b), Combi lipid (c), Phospholipon® 90H (d), Blank-SLNs (e), INH-SLNs (d).

The absence of or weakening of Phospholipon® 90H signal indicates a strong interaction of its functional groups with the solid Combi lipid as observed in the mobility of its functional group. This reduced or no signal in contrast to the strong signal for Tween 80 in INH-SLNs indicates its attachment but not incorporation into the lipid core material, since a weak signal is still observed [31]. The surfactant tail groups in the lipid emulsion are likely to be packed tightly together at the oil–water interface, thus forming a relatively rigid ‘‘shell” surrounding the encapsulated lipid droplets at high surfactant concentrations as for Tween 80 (27 %) in presently prepared INH-SLNs using microemulsification technique. In such cases, the surfactant restricts the molecular motion of the triacylglycerol molecules of the lipid within the droplet interior [32]. However, Tween 80 shows a distinct peak in the NMR spectra of INH-SLNs indicating its presence in the shell and may be in the outer aqueous region as free surfactant due to its higher concentration.

Cytotoxicity studies

Cytotoxicity of the developed formulation was checked in both HCJE and HCLE cell lines. The concentration of 1 µg/ml and 10 µg/ml was selected for the study. No statistically significant ($P<0.05$) cytotoxicity was observed for Blank-SLNs and INH-SLNs in comparison to control when administered to HCJE and HCLE cells at these concentrations after incubation for 24 h (Figure S9).

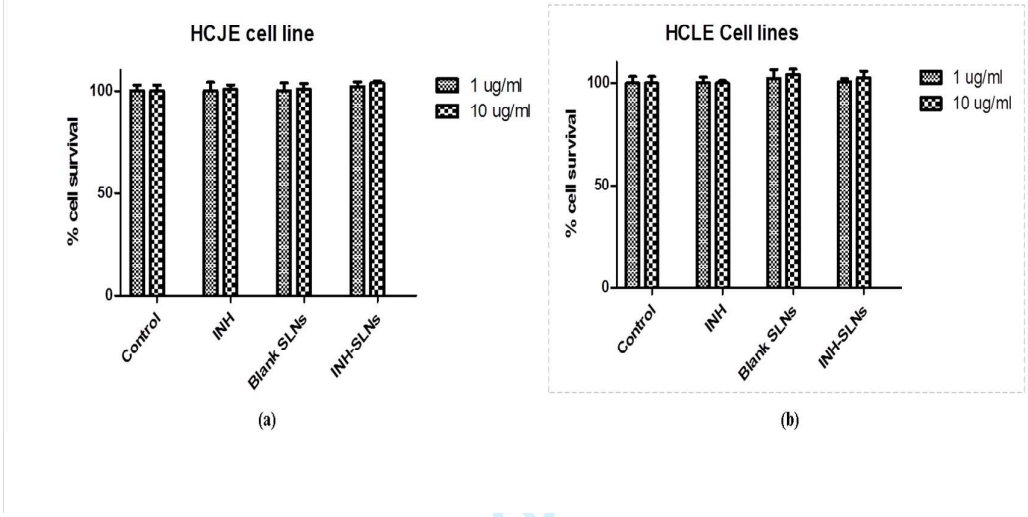

Figure S9: % Cell viability in HCJE and HCLE cells at varying concentration after incubation for 24 h.

Dermal irritation studies

The score for dermal irritation/corrosion study are compiled in Table 2. Figure S10 shows the skin of test animals, photographed before and after application of the formulation. Zero scores clearly demonstrate a non-irritating/corrosive nature of developed SLNs when applied to dermal tissues, and hence we proceeded to the eye irritation test (section 3.5) in accordance with OECD guidelines.

(a) (b)

Figure S10 Skin surface of rabbit (a) before application of the formulation and (b) after application.

Table S2: Acute dermal irritation/corrosion study of INH-SLNs in rabbits.

DERMAL	Scores of rabbit 1					Scores of rabbit 2					Scores of rabbit 3					Score
	Time (h)															
	0 h	**1 h**	**24 h**	**48 h**	**72 h**	**0 h**	**1 h**	**24 h**	**48 h**	**72 h**	**0 h**	**1 h**	**24 h**	**48 h**	**72 h**	
Erythmea	0	0	0	0	0	0	0	0	0	0	0	0	0	0	0	**0/40**
Odema	0	0	0	0	0	0	0	0	0	0	0	0	0	0	0	**0/40**
Total score																**0/80**

Acute eye irritation/corrosion test

Single instillation study

Zero scores established that developed SLN system is safe for ocular delivery after single instillation (Table 3). There were no sign of irritation/corrosion in any ocular tissue.

Table S3: Single instillation acute eye irritation/corrosion study of INH-SLNs in rabbit eye.

Ocular tissue	Scores of rabbit 1					Scores of rabbit 2					Scores of rabbit 3					Score
	Time (h)															
	0 h	1 h	24 h	48 h	72 h	0 h	1 h	24 h	48 h	72 h	0 h	1 h	24 h	48 h	72 h	
Cornea	0	0	0	0	0	0	0	0	0	0	0	0	0	0	0	0/60
Iris	0	0	0	0	0	0	0	0	0	0	0	0	0	0	0	0/30
Conjunctiva	0	0	0	0	0	0	0	0	0	0	0	0	1	1	0	0/45
Chemosis	0	0	0	0	0	0	0	0	0	0	0	0	0	0	0	0/60
Total score																**0/195**

Repeated instillation study

This study is a modification or extension of the previous study and was performed in view of the fact that it is usually recommended to frequently repeat the instillation of ocular formulations. Similar studies have been reported by us earlier [33]. The zero scores obtained from this study (Table S4) prove the system to be safe for repetitive ocular use too.

Table S4: Repeat instillation acute eye irritation/corrosion study of INH-SLNs in rabbit eye.

Ocular tissue	Scores of rabbit 1					Scores of rabbit 2					Scores of rabbit 3					Score
	Time (h)															
	0 h	1 h	24 h	48 h	72 h	0 h	1 h	24 h	48 h	72 h	0 h	1 h	24 h	48 h	72 h	
Cornea	0	0	0	0	0	0	0	0	0	0	0	0	0	0	0	0/60
Iris	0	0	0	0	0	0	0	0	0	0	0	0	0	0	0	0/30
Conjunctiva	0	0	0	0	0	0	0	0	0	0	0	0	1	1	0	0/45
Chemosis	0	0	0	0	0	0	0	0	0	0	0	0	0	0	0	0/60
Total score																**0/195**

Chronic repeat instillation irritation/corrosion test

The treatment of Mycobacterium infection may involve therapy for longer periods, so we evaluated the developed formulation for chronic repeat instillation (5 times at 5 minute interval) for a period of one week. Compilation of scores (zero value) demonstrate the SLN disperse system to be non-irritant/corrosive upon chronic use for upto 7 days to all ocular tissues, and are concluded to be safe for chronic ocular use (Table S5).

Table S5: Scores of chronic repeat instillation irritation/corrosion study INH-SLNs

Ocular tissue		Cornea	Iris	Conjunctiva	Chemosis	Score	Total Score
rabbit 1	0h	0	0	0	0	0/104	0/312
	1d	0	0	0	0		
	2d	0	0	0	0		
	3d	0	0	0	0		
	5d	0	0	0	0		
	6d	0	0	0	0		
	7d	0	0	0	0		
rabbit 2	0h	0	0	0	0	0/104	
	1d	0	0	0	0		
	2d	0	0	0	0		
	3d	0	0	0	0		
	5d	0	0	0	0		
	6d	0	0	0	0		
	7d	0	0	0	0		
rabbit 3	0h	0	0	0	0	0/104	
	1d	0	0	0	0		
	2d	0	0	0	0		
	3d	0	0	0	0		
	5d	0	0	0	0		
	6d	0	0	0	0		
	7d	0	0	0	0		

Ocular safety studies of the developed system were performed to evaluate its efficacy by using cell viability assays, histological studies and in vivo experiments. Due to more

common anatomical and biochemical features of rabbits eye with human eye, it was used as the animal of choice [34].

Ocular tolerance evaluation

Corneal, retinal and conjunctival cross-sections were evaluated, post administration of INH-SLNs in rat eyes for their influence, if any, on cell structure and tissue integrity. Results confirmed absence of any adverse effects on tissue integrity. The tissue appeared normal and no signs of inflammation such as accumulation of macrophages, and lymphocytic infiltrate were observed (Fig.13). The developed formulation left the tissue structure and integrity visibly unaffected. Results confirm good ocular biocompatibility of the developed formulation.

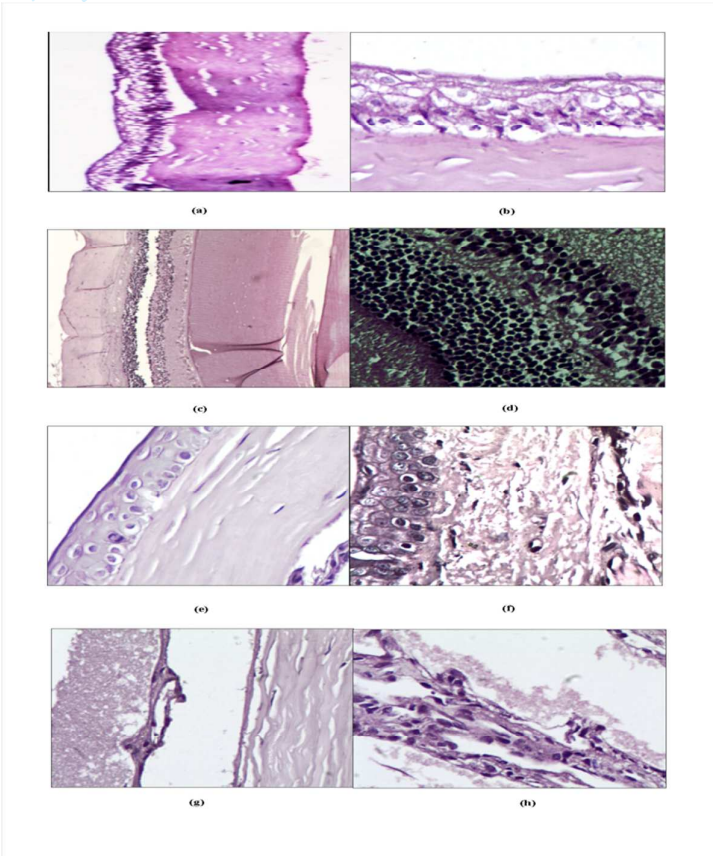

Figure S11: Optical microscopic pictures showing histological section of rat eye

Naïve control represented in (a) retina and sclera at 10X (b) at 40X. (c)- (h) represent conjunctival tissue of test animals at 30 min (c and d), 1 h (e and f) and 2 h (g and h).

References

Kakkar S, Karuppayil SM, Raut JS, et al., **Lipid-polyethylene glycol based nano-ocular formulation of ketoconazole**. *Int J Pharm*. 2015;495:276-289

Gipson IK, Michaud SS, Argueso P, et al., **Mucin gene expression in immortalized human corneal-limbal and conjunctival epithelial cell lines.** *Invest Ophthalmol Vis Sci.* 2003;44:2496-2506

Guzman-Aranguez A, Calvo P, Ropero I and Pintor J, **In vitro effects of preserved and unpreserved anti-allergic drugs on human corneal epithelial cells.** *J Ocul Pharmacol Ther*. 2014;30:790-798

OECD, 2015. *Test No. 404: Acute Dermal Irritation/Corrosion*, OECD Paris.

OECD, 2017. *Test No. 405: Acute Eye Irritation/Corrosion*, OECD, Paris.

Bhandari R and Kaur IP, **A Method to Prepare Solid Lipid Nanoparticles with Improved Entrapment Efficiency of Hydrophilic Drugs** *Curr Nanosci*. 2013;9:211-220

Hironaka K, Inokuchi Y, Tozuka Y, et al., **Design and evaluation of a liposomal delivery system targeting the posterior segment of the eye**. *J Control Release*. 2009;136:247-253

Yoncheva K, Lizarraga E and Irache JM, **Pegylated nanoparticles based on poly(methyl vinyl ether-co-maleic anhydride): preparation and evaluation of their bioadhesive properties**. *Eur J Pharm Sci*. 2005;24:411-419

Shen Y and Tu J, **Preparation and ocular pharmacokinetics of ganciclovir liposomes**. *AAPS J*. 2007;9:1-7

Nagarwal RC, Kant S, Singh PN, Maiti P and Pandit JK, **Polymeric nanoparticulate system: a potential approach for ocular drug delivery**. *J Control Release*. 2009;136:2-13

Alany RG, Rades T, Nicoll J, Tucker IG and Davies NM, **W/O microemulsions for ocular delivery: evaluation of ocular irritation and precorneal retention**. *J Control Release*. 2006;111:145-152

Shah RM, Eldridge DS, Palombo EA and Harding IH, **Microwave-assisted formulation of solid lipid nanoparticles loaded with non-steroidal anti-inflammatory drugs**. *Int J Pharm*. 2016;515:543-554

Missana T and Adell A, **On the applicability of DLVO theory to the prediction of clay colloids stability**. *J Colloid Interface Sci.* 2000;230:150-156

Singh H, Bhandari R and Kaur IP, **Encapsulation of Rifampicin in a solid lipid nanoparticulate system to limit its degradation and interaction with Isoniazid at acidic pH**. *Int J Pharm*. 2013;446:106-111

Choi KO, Aditya NP and Ko S, **Effect of aqueous pH and electrolyte concentration on structure, stability and flow behavior of non-ionic surfactant based solid lipid nanoparticles**. *Food Chem*. 2014;147:239-244

Liu Y, Liu J, Zhang X, et al., **In situ gelling gelrite/alginate formulations as vehicles for ophthalmic drug delivery**. *AAPS PharmSciTech*. 2010;11:610-620

Cui Z, Shi KZ, Cui YZ and Binks BP, **Double phase inversion of emulsions stabilized by a mixture of $CaCO_3$ nanoparticles and sodium dodecyl sulphate**. *Colloids Surf A Physicochem Eng Asp*. 2008;329:67-74

Freitas C and Müller RH, **Stability determination of solid lipid nanoparticles (SLN) in aqueous dispersion after addition of electrolyte**. *J Microencapsul*. 1999;16:59-71

Dubes A, Lopez HP, Abdelwahed W, et al., **Scanning electron microscopy and atomic force microscopy imaging of solid lipid nanoparticles derived from amphiphilic cyclodextrins**. *Eur J Pharm Biopharm*. 2003;55:279-282

Damari SP, Shamrakov D, Varenik M, et al., **Practical aspects in size and morphology characterization of drug-loaded nano-liposomes**. *Int J Pharm*. 2018;547:648-655

Li Y, Kroger M and Liu WK, **Shape effect in cellular uptake of PEGylated nanoparticles: comparison between sphere, rod, cube and disk**. *Nanoscale*. 2015;7:16631-16646

Bunjes H, Steiniger F and Richter W, **Visualizing the structure of triglyceride nanoparticles in different crystal modifications**. *Langmuir*. 2007;23:4005-4011

Brubach JB, Jannin V, Mahler B, et al., **Structural and thermal characterization of glyceryl behenate by X-ray diffraction coupled to differential calorimetry and infrared spectroscopy**. *Int J Pharm*. 2007;336:248-256

Lewis RNAH and McElhaney RN, **Membrane lipid phase transitions and phase organization studied by Fourier transform infrared spectroscopy**. *Biochim Biophys Acta*. 2013;1828:2347-2358

Bunjes H and Unruh T, **Characterization of lipid nanoparticles by differential scanning calorimetry, X-ray and neutron scattering** *Adv Drug Deliv Rev*. 2007;59:379–402

Unruh T, Bunjes H, Westesen K and Koch MHJ, **Investigations on the melting behaviour of triglyceride nanoparticles**. *Colloid Polym Sci*. 2001;279:398-403

Bunjes H, Koch MHJ and Westesen K, **Effect of Particle Size on Colloidal Solid Triglycerides**. *Langmuir*. 2000;16:5234-5241

Hunter RJ, **Foundations of Colloid Science**. *Clarendon Press, Oxford*. 1993;1:267–269

Westesen K, Bunjes H and Koch MHJ, **Physicochemical characterization of lipid nanoparticles and evaluation of their drug loading capacity and sustained release potential**. *J Control Release*. 1997;48:223-236

Ali H, El-Sayed K, Sylvester PW and Nazzal S, **Molecular interaction and localization of tocotrienol-rich fraction (TRF) within the matrices of lipid nanoparticles: Evidence studies by Differential Scanning Calorimetry (DSC) and Proton Nuclear Magnetic Resonance spectroscopy (^{1}H NMR)**. *Colloids Surf B Biointerfaces*. 2010;77:286-297

Schubert MA, Harms M and Müller-Goymann CC, **Structural investigations on lipid nanoparticles containing high amounts of lecithin**. *Eur J Pharm Sci*. 2006;27:226-236

Helgason T, Awad TS, Kristbergsson K, McClements DJ and Weiss J, **Effect of surfactant surface coverage on formation of solid lipid nanoparticles (SLN)**. *J Colloid Interface Sci*. 2009;334:75-81

Kaur IP and Kakkar S, **Nanotherapy for posterior eye diseases**. *J Control Release*. 2014;193:100-112

Zernii EY, Baksheeva VE, Iomdina EN, et al., **Rabbit Models of Ocular Diseases: New Relevance for Classical Approaches**. *CNS Neurol Disord Drug Targets.* 2016;15:267-291